Protein environment and structure in neat and hydrated deep eutectic solvents

LUNDS UNIVERSITET

A master's thesis by
Jenny Xiang and Medina Basic

Supervisor
Dr. Adrian Sanchez Fernandez
Department of Food Technology, Engineering and Nutrition
Lund University

Examiner
Prof. Marie Wahlgren
Department of Food Technology, Engineering and Nutrition
Lund University

Monday, 15 June 2020

Populärvetenskaplig sammanfattning

Ett arbete som som syftar till att studera hur djupa eutektiska lösningsmedel påverkar proteinerna bovin serumalbumin och lysozym

Ett djupt eutektiskt lösningsmedel är ett lösningsmedel som skapas när två eller fler fasta material, mer specifikt en vätebindningsacceptor (ofta ett kvartärt ammoniumsalt) och en vätebindningsdonator, bildar ett omfattande vätebindningsnätverk. Detta genererar en eutektisk blandning i flytande form när de blandas i rätt förhållanden. Dessa lösningsmedel är klassade som grönare lösningsmedel som är icke-toxiska, nedbrytbara och biokompatibla, vilket gör de intressanta inom olika användningsområden. De eutektiska blandningarna skulle t.ex. potentiellt kunna användas som medium för proteiner. Proteiner består av långa kedjor av aminosyror med olika egenskaper som är kombinerade på olika sätt för att bilda långa kedjor som resulterar i ett specifikt protein med en särskild struktur och funktion.

De två proteinerna som studerats i denna studie är bovin serumalbumin och lysozym. Bovin serumalbumin är ett protein härrörande från kor som har studerats omfattande på grund av dess tillgänglighet, låga kostnad, stabilitet och förmåga att inte skapa korsreaktioner i många biologiska reaktioner. Lysozym är ett annat protein som finns hos djur (proteinet utvinns ofta från kyckling- eller hönsäggvita) och i t.ex. slemhinnor, tårar, saliv etc. Proteinet, som också är ett enzym, är känt för sin antibakteriella aktivitet.

I detta arbete har det med hjälp av olika analysmetoder studerats hur dessa två proteiner påverkas av tre olika eutektiska lösningsmedel. Bland annat har koncentrationen av protein samt förändring av proteinets miljö observerats när respektive protein befinner sig i respektive lösningsmedel. Erhållna resultat har sedan jämförts med resultat från när respektive protein befinner sig i fosfatbuffert. Spektroskopiska analysmetoder har använts för att titta på hur proteinstrukturen påverkas. Dessutom har det även studerats hur proteinet reagerar på tillsatsen av vatten till den eutektiska lösningen (då det tidigare har observerats att detta kan vara fördelaktigt för proteinets struktur) samt hur proteinet förändrats när den förflyttas till fosfatbuffert igen efter att ha varit i den eutektiska lösningen under en viss tid.

Den slutsats som kan dras av arbetet är att den ursprungliga proteinstrukturen av BSA och lysozym med stor sannolikhet har förändrats när proteinerna har introducerats till de olika djupa eutektiska lösningsmedlen, samt att olika utfall fås beroende på vilket eutektiskt lösningsmedel proteinet förts in i. Resultaten har även visat att proteinerna behåller sina strukturer bättre i de eutektiska lösningarna om vatten tillsätts, samt att merparten av proteinstrukturen återgår till original form när proteinet återförs till fosfatbuffert från den eutektiska lösningen.

Acknowledgement

We would like to begin with thanking Professor Marie Wahlgren for enabling us to perform our master thesis at the department and in this study field. The outcome of this master thesis would not have been the same without our supervisor, Dr. Adrian Sanchez Fernandez, who has provided us with important knowledge and insights as well as support, throughout the experimental work and the report writing. Further on we would like to sincerely thank Assoc. Prof. Cedric Dicko, that has introduced us to the FT-IR and fluorescence spectrometers, and spent a lot of time helping us to interpret the obtained data that were not always the easiest to understand. We would also like to thank Olexandr Fedkiv (project assistant at Department of Food Technology, Engineering and Nutrition) and research engineer Hans Bolinsson for their help and patience when providing us with knowledge regarding the different instruments (e.g. freeze drier and vacuum drier) at the department as well helping us through other smaller obstacles that we faced throughout the laboratory work. Lastly, a big Thank you to everyone at the Department of Food Technology, Engineering and Nutrition for providing us with a welcoming and good working environment that kept motivating us to move forward in our project.

With this thesis we have gained a lot of knowledge and experience within the research field. It has been a pleasure undertaking this task and solving the problems that were encountered and this would not have been as entertaining without each other. A lot of hard work has been put into the experimental work, analysis of data and report writing. Despite this, a lot of laughter has been shared and to this we have each other to thank. This thesis would not have been the same without our good team spirit and support, especially during times when our email inboxes as well as the department stood empty. On a more serious note, Thank you all for being a part of this journey, it has been a wonderful last semester at Lund University, marking the end of our education as Masters of Science in Engineering, Biotechnology.

Abbreviations

BSA	- bovine serum albumin
BSA100	- BSA in a concentration of 100 μM
BSA50	- BSA in a concentration of 50 μM
BSA10	- BSA in a concentration of 10 μM
CD	- circular dichroism
ChAc	- choline acetate
ChCl	- choline chloride
DES	- deep eutectic solvent
FT-IR	- Fourier transform-infrared
Gly	- glycerol
HD ChCl:Gly	- hydrated choline chloride:glycerol
HD DESs	- hydrated deep eutectic solvents
Lys	- lysozyme
Lys100	- lysozyme in a concentration of 100 μM
Lys50	- lysozyme in a concentration of 50 μM
Lys10	- lysozyme in a concentration of 10 μM
Phe	- phenylalanine
SANS	- small-angle neutron scattering
SAXS	- small-angle x-ray scattering
Trp	- tryptophan
Tyr	- tyrosine
U	- urea
UV	- ultraviolet

Abstract

The use of deep eutectic solvents (DESs) has a great potential in the pharmaceutical field due to its many advantages such as biocompatibility, low toxicity and biodegradability. Studies have also shown that proteins can be successfully incorporated into DESs. However, protein stability and structure in these solvents need to be investigated for this technology to be applicable. When adding the protein into the deep eutectic solvent, the sought outcome is not to disrupt the native protein conformation, but to stabilize the protein in the solvent. A factor that makes this difficult is that proteins can change their structure when the local environment of the amino acid residues of the protein is altered.

In this thesis, the two proteins bovine serum albumin and lysozyme were studied in three different DESs; choline chloride:glycerol (ChCl:Gly), choline chloride:urea (ChCl:U) and choline acetate:glycerol (ChAc:Gly), all in the molar ratio 1:2. In order to evaluate protein concentration, monitor changes in the secondary structure and how the environment affects the protein, UV-Vis spectrometry, FT-IR and fluorescence spectroscopy have been utilized. Hydrated ChCl:Gly with incorporated proteins has also been studied to understand how the proteins respond to the addition of water in the DES. Finally, proteins in ChCl:Gly were back-extracted into phosphate buffer to see how the proteins behave after being exposed to DES and then transferred back into a neat aqueous environment.

From the UV-Vis measurements, the obtained data indicate that the conformation of BSA and lysozyme seems to be best retained in ChCl:Gly. The FT-IR measurements show that the secondary structure is altered for the proteins when they are in DESs. Moreover, the data from the fluorescence measurements suggests that the native conformation of BSA and lysozyme, the environment or the interactions with the environment most likely is altered when the proteins are introduced to the different DESs. Furthermore, when adding water to ChCl:Gly, the protein conformations are better retained compared to when the proteins are in pure ChCl:Gly. After extraction of proteins from ChCl:Gly to phosphate buffer, it is observed that the proteins regain most of their native conformation. Consequently, deep eutectic solvents might be applicable in drug formulation. However, more studies have to be performed (preferably in combination with other techniques enabling further conformational studies) to obtain complementing information.

Sammanfattning

Användningen av djupa eutektiska lösningsmedel har en stor potential i läkemedelsbranschen på grund av deras många fördelar som exempelvis biokompabilitet, låg toxicitet och bionedbrytbarhet. Studier har visat att proteiner med framgång kan föras in i djupa eutektiska lösningsmedel men för att detta ska bli applicerbart måste proteinstabilitet och proteinstruktur studeras i dessa lösningsmedel. När man för in protein i de eutektiska lösningsmedlen är det önskade utfallet inte att proteinets ursprungliga struktur drastiskt förändras, utan istället stabiliseras i det nya mediet. En faktor som gör detta svårt är att proteiners struktur kan förändras när den lokala miljön av proteinets aminosyror förändras.

I detta arbete har två proteiner, bovin serumalbumin och lysozym, studerats i tre olika eutektiska lösningsmedel; kolinklorid:glycerol, kolinklorid:urea och kolinacetat:glycerol, alla i molförhållandet 1:2. I syfte att evaluera proteinkoncentration, observera förändringar i sekundärstruktur och hur miljön påverkar proteinet har UV-Vis spektrometri, FT-IR- och fluorescensspektroskopi använts. Även hydrerade djupa eutektiska lösningsmedel har studerats med avsikten att förstå proteiners respons till tillsatsen av vatten i de eutektiska lösningsmedlen. Dessutom har proteinerna återextraherats till fosfatbuffert för att se hur proteiner beter sig efter att ha exponerats för djupa eutektiska lösningsmedel och därefter förs tillbaka till en vattenfas.

Från UV-Vis mätningarna indikerar erhållen data att konformationen av BSA och lysozym verkar bevaras bäst i kolinklorid:glycerol. Från FT-IR mätningarna kan man se att sekundärstrukturen av proteinerna förändras när de befinner sig i de olika djupa eutektiska lösningsmedlen. Resultaten från fluorescensmätningarna indikerar att den ursprungliga konformationen av BSA och lysozym, miljön eller interaktionerna med miljön med stor sannolikhet förändras när proteinerna förs in i de olika djupa eutektiska lösningsmedlen. När vatten tillsätts till kolinklorid:glycerol visar det sig att proteinkonformationerna bevaras bättre jämfört med när proteinerna är i ren kolinklorid:glycerol. Vidare observerades det att efter extrahering av proteiner från kolinklorid:glycerol till fosfatbuffert återfår proteinerna mestadels av sin ursprungliga konformation. För att sammanfatta så har djupa eutektiska lösningsmedel potential inom läkemedelsformulering, men fler studier måste utföras (i synnerhet i kombination av andra tekniker, vilka möjliggör ytterligare konformationsstudier) i syfte att erhålla komplementär information.

Table of content

1. Introduction 8
1.1. Aim 8
1.2. Division of work 8
2. Background and theory 9
2.1. DESs 9
2.1.1. Applications of DESs 9
2.1.2. Hydrated DESs 10
2.2. Proteins 11
2.2.1. Protein structure 11
2.2.2. Unfolding of proteins 11
2.2.3. BSA 11
2.2.4. Lysozyme 12
3. Analysis methods 12
3.1. UV-Vis spectrometry 12
3.1.1. Uses of derivative spectroscopy 12
3.2. FT-IR spectroscopy (Fourier transform-infrared spectroscopy) 13
3.3. Fluorescence spectroscopy 13
4. Materials and methods 14
4.1. Materials 14
4.2. Methods 14
4.2.1. Preparation of the DESs and protein samples 14
4.2.2. Experimental setup 15
5. Results and discussion 16
5.1. NanoDrop measurements 16
5.2. Neat DESs: UV-Vis measurements 16
5.2.1. ChCl:Gly 18
5.2.2. ChCl:U 18
5.2.3. ChAc:Gly 18
5.2.4. Comparison of BSA and lysozyme in all three DESs and buffer 19
5.3. Neat DESs: FT-IR measurements 19
5.4. Neat DESs: Fluorescence measurements 22
5.5. Hydrated DES 25
5.5.1. HD DES: UV-Vis measurements 25
5.5.2. HD DES: FT-IR measurements 26
5.5.3. HD DES: Fluorescence measurements 26
5.6. Extracted proteins 28
5.6.1. Extracted proteins: UV-Vis measurements 28
5.6.2. Extracted proteins: FT-IR measurements 30
5.6.3. Extracted proteins: Fluorescence measurements 31
6. Conclusion 32
7. Future outlook 32
8. References 33
9. Appendices 36

1. Introduction

Deep eutectic solvents (DESs) are relatively new kinds of solvents with properties similar to ionic liquids. Their many advantages, e.g. low toxicity, biodegradability, biocompatibility and low vapour pressure, make them usable in applications like biosynthesis, organic synthesis and enzymatic reactions etc. and they constitute a green alternative compared to traditional organic solvents (Zhang et al., 2012).

One interesting area where DESs can be useful is the pharmaceutical field. Due to the biocompatibility and low toxicity, DESs make great potential as drug carriers. However, for this to be applicable protein stability and structure need to be investigated in DESs in order to make sure that the active pharmaceutical ingredient can exert its effects when delivered to the target site. When adding the protein into the deep eutectic solvent, the wanted outcome is not to disrupt the native protein conformation, but to stabilize the protein in the solvent. However, it is known that the protein can change its structure when the local environment of the constituent amino acids is altered. It is therefore of importance to understand protein behavior, and how protein conformation and folding is affected when the macromolecule is exposed to the deep eutectic solvent.

1.1. Aim

The aim is to investigate how different deep eutectic solvents affect the protein structure. In order to do this, methods have to be developed to incorporate the proteins into water-free DESs in a way that the samples become homogeneous. Furthermore, the effect of water addition to the DESs/protein samples will be investigated as well as the recovery of protein structure when being back-extracted into water solution. In this study, DESs with different key properties are selected. Choline chloride and choline acetate will be studied with the aim to understand the effect of the counterion to choline. Additionally, the two chosen hydrogen bond donors are glycerol and urea. Urea is known to be a protein denaturant while glycerol often is used to stabilize proteins in solutions. The properties of the two different donors will be evaluated when these are utilized to create the DESs.

1.2. Division of work

An approach for incorporating the protein into the DESs were developed together. The work of incorporation of the proteins in the three different DESs and phosphate buffer and measurements of the samples with the different techniques was split equally between the two analysts. This offered the opportunity to operate all the different techniques for both analysts. However, the UV-Vis and NanoDrop measurements were often run simultaneously, which resulted in that one analyst was more dedicated to the UV-Vis while the other operated the NanoDrop more frequently. Preparation of hydrated DES samples and extraction of protein were executed together, while measurements of these samples with the different techniques were performed separately. Nonetheless, both analysts again got the chance to operate all of the different instruments. Furthermore, the report writing was divided equally between the two persons and thoroughly revised by the two authors. The majority of the parts before section “5. Results and discussion” were written by one person, while the other person focused more on plotting of the graphs in excel and MagicPlot.

2. Background and theory

2.1. DESs

A deep eutectic solvent is a liquid that is formed when two or more solids are mixed together in a specific molar ratio. The two solids, one hydrogen bond acceptor (often quaternary ammonium salt) and one hydrogen bond donor, interact and form an extensive hydrogen bond network creating the eutectic mixture. The hydrogen bond is formed between the DES constituents and allow this to remain stable and in a highly entropic state (Hammond, Bowron and Edler, 2016). Depending on the combination of hydrogen bond acceptor and hydrogen bond donor, the melting point of the eutectic mixture differs, but normally the melting point of a deep eutectic solvent is below room temperature (Zhang et al., 2012). The freezing point of the formed DES is lower than the melting point of each individual component (often more than 150 °C lower) and this is suggested to be due to the strong hydrogen bonds formed between the two components, hindering crystallization of the salt (Abbott et al., 2003), or the charge delocalization occurring when the two components complex (Esquembre et al., 2013; Gutiérrez et al., 2010).

In this thesis, the two proteins bovine serum albumin (BSA) and lysozyme were studied in three different DESs; choline chloride:glycerol (ChCl:Gly), choline chloride:urea (ChCl:U) and choline acetate:glycerol (ChAc:Gly), all in the molar ratios 1:2 (one mole of quaternary ammonium salt to two moles of hydrogen bond donor). The structures of the two quaternary ammonium salts, choline chloride and choline acetate, and the two hydrogen bond donors glycerol and urea can be seen in *Figure 1*.

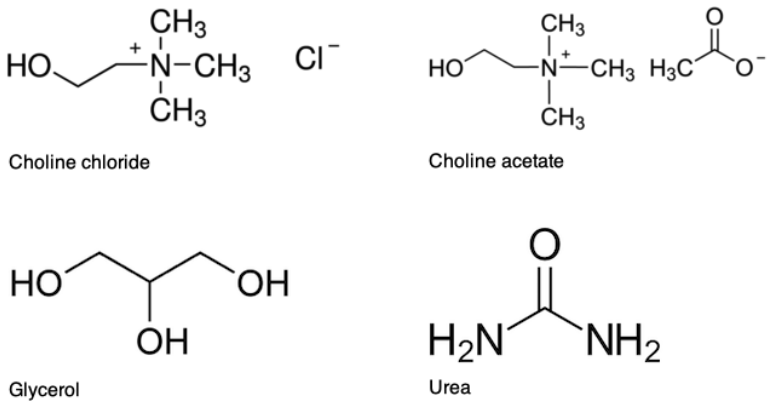

***Figure 1**. Chemical structures of choline chloride, choline acetate, glycerol and urea. Hydrogen bonding occurs between the hydrogen bond donor and the anion of the hydrogen bond acceptor, creating the deep eutectic solvent.*

2.1.1. Applications of DESs

DESs have started to become more common as solvents in synthesis due to being more environmentally friendly compared to the traditional organic solvents utilized for synthesis. They have for example been helpful in selective N-alkylation reactions of aromatic primary amines where polar organic solvents often can lead to more than one alkylation. Hence, a more selective alkylation can be achieved with DESs (Smith, Abbott and Ryder, 2014). One particular study showed that DESs (ChCl:U and ChCl:Gly, both in a molar ratio of 1:2) could be recycled five times when being used for the N-alkylation of the aromatic primary amines, where the catalytic activity of the DESs only was reduced to a small extent (Singh, Lobo and Shankarling, 2011). Furthermore, the synthesis of cinnamic acid normally requires strong bases, organic solvents and high reaction temperatures and this can be avoided with the utilization of ChCl:U, which allows reactions to occur at substantially lower reaction temperatures and result in higher yields of the desired product (Pawar, Jarag and Shankarling, 2011). Besides synthesis, DESs are useful in other fields such as in metal processing. Traditional solvents used in metal electropolishing are aqueous based but the problems with these are that they can be toxic and corrosive and that these processes usually involve great gas development, leading to lower current efficiencies. The benefits with using DESs in these applications are that the gas development is insignificant and that the solutions are

non-harmful and do not cause corrosion (Smith, Abbott and Ryder, 2014). Furthermore, studies have been made on ChCl:U in drug solubilization applications, showing that the DES had significantly greater drug solubility than water. The macromolecule AMG517 had a solubility of less than 0.0001 mg/mL in pure water compared to 0.01 mg/mL in pure ChCl:U. However, more studies need to be done on the solubility of drugs in DESs to confirm the advantages of DESs regarding the enhanced solubility of the macromolecules (Zhang et al., 2012).

DESs also have the ability to separate the remaining glycerol that is formed as a byproduct during the production of biodiesel, which occurs through the transesterification of triglyceride oils. Different approaches have been utilized for the separation of glycerol from biodiesel and there is a constant search for more economically favorable methods. As such, eutectic mixtures with glycerol have shown potential in facilitating the purification (Abbott et al., 2007; Zhang et al., 2012). One study investigated how a eutectic mixture (1:1 ratio of quaternary ammonium salt and glycerol) was added to biodiesel containing glycerol. The additional glycerol resulted in a eutectic mixture between the quaternary salt and glycerol in a molar ratio of 1:2, which allowed a significant removal of glycerol in the biodiesel (Abbott et al., 2007). Moreover, another application that DESs have shown potential in is in catalysis reactions. Studies have shown that DESs enhance the reaction rates through the stabilization of transition states. One advantage making them more desirable for use in catalysis is that they can be recycled for several cycles (Zhang et al., 2012).

2.1.2. Hydrated DESs

The ability of the DES components to form hydrogen bonds generally makes these eutectic solvents hygroscopic and water-miscible. When not stored properly, they absorb water from the air and this may unfavorably alter the physicochemical properties of the DES. However, water can also be added intentionally to these systems, taking advantage of the possibility to change the properties of the DES. Depending on the amount of water added, the structure of the eutectic mixtures will change to different degrees and when a sufficiently high amount of water has been added, the system ultimately becomes an aqueous solution of the components of the DES (Hammond, Bowron and Edler, 2017). The interactions between the different DES components will gradually, but non-linearly, weaken as more and more water is added, while the interactions between the components and water will increase. In a ChCl:U deep eutectic solvent with up to approximately 40 wt% water, the water will be mostly sequestered around the choline cations, which can explain the low water activity observed in hydrated DES systems (Dai et al., 2013; Hammond, Bowron and Edler, 2017). At approximately 50 wt% water and above, the DES/Water system is no longer considered as a hydrated DES, but rather an aqueous solution of DES components. This is due to the fact that water molecules surround and interact with the individual DES components at shorter distances compared to the component-component distances. The water-DES component interactions dominate over the DES-DES interactions (that still exist to a smaller extent) above this point and additional water addition only increases the solvation of the DES components (Hammond, Bowron and Edler, 2017). For other deep eutectic solvents, the same weakening of the DES-DES interactions and strengthening of water-DES interactions are potentially seen, but the point where the change from a hydrated DES to an aqueous solution is reached might be different.

One advantage of hydrated DES compared to pure DES is the lower viscosity, decreasing the mass transfer resistance of the system. Furthermore, water can be added to increase the solubility and availability of substrates that are used for synthetic purposes in DES systems. The extensive hydrogen bonding network in DES systems and the ability of water molecules to hydrogen bond also lowers the reactivity of water in these water/DES systems, decreasing unfavorable hydrolysis reactions and other unwanted side reactions. Water activity is an important parameter when it comes to the activity of enzymes since it determines the hydration state of the enzymes. It has been shown for ChCl:U and ChCl:Gly DESs that the water activity is linearly proportional to the water content added and that the proportionality constant is the same for both DESs, indicating that the choline chloride is more important for the water activity of the system than the hydrogen bond donor. Additionally, the stability of enzymes can be increased in hydrated DESs compared to pure DESs (Durand et al., 2013).

2.2. Proteins

2.2.1. Protein structure

There are four hierarchical levels of protein structure that are distinguished by the level of complexity in the polypeptide chain. The primary structure of a protein is its amino acid sequence, which starts at the N-terminal and ends at the C-terminal. The regular pattern formed on the polypeptide backbone chain, which is stabilized due to hydrogen bonds between amino- and keto groups of the peptide bonds, defines the secondary structure. The main patterns in the secondary structure are the alpha-helices and beta-sheets (Buxbaum, 2015). The tertiary structure is the three-dimensional constitution of the polypeptide chain, which is determined by interactions (that can occur between amino acid residues that are far apart from each other) such as hydrogen bonding, van der Waals interactions, hydrophobic interactions, salt bridges and disulfide bridges. In aqueous environments, it is more thermodynamically favorable when the hydrophobic side chains of the polypeptide form the core of the protein whereas the hydrophilic side chains are found on the surface of the protein (Berg et al., 2015). The fourth level of the protein structure, the quaternary structure, emerges when more than one polypeptide chain associate into a single 3D structure, where each polypeptide chain is referred to as a subunit. Hence, the quaternary structure is defined by the interactions between the different subunits and their overall three-dimensional structure (Berg et al., 2015; Buxbaum, 2015).

2.2.2. Unfolding of proteins

The distribution of polar and nonpolar amino acids in proteins has a big impact on protein folding and this folding will be influenced by the environment of these residues. In a hydrophilic solution, the polar and charged residues will be exposed to the hydrophilic environment whereas the hydrophobic residues will be clustered together on the inside of the protein. When the local environment of the amino acids is altered, the protein conformation can be affected and result in a disrupted protein (Berg et al., 2015).

It has been noted that denaturation of protein can occur through chemical-, temperature-, force- and pressure effects. Two known chemical denaturants are guanidine hydrochloride and urea. Both have a low molecular weight and high solubility, where concentrations of 6-8 M are needed to be able to denature proteins. For urea, it has been shown that this molecule interacts with the backbone of polypeptides by hydrogen bond interactions, leading to the disruption of the native protein structure. The guanidine hydrochloride, however, disrupts the hydrophobic interactions in the native protein (Lapidus, 2017). Despite urea being a protein denaturant, studies have been made on enzymes such as *Candida antarctica* lipase B, indicating that the enzyme activity and stability is retained in deep eutectic solvents containing high contents of urea (66%). The same enzyme denatured completely with a content of 12% of urea (8M) in water. The reason why the enzyme was not denatured in the DES with a higher content of urea is that the diffusion coefficient of urea is smaller in the DES, making it harder for urea to disrupt the intrachain hydrogen bonds of the protein. The smaller diffusion coefficient of urea was in turn associated to that urea forms hydrogen bonds to the choline and chloride ions present (Monhemi et al., 2014).

2.2.3. BSA

Bovine serum albumin (BSA) with a molecular weight of 66 kDa and a pI of 4.7, is a globular protein that is widely used as model systems due to its stability, availability, low cost and ability of not causing cross reactions in many biological reactions. It is composed of one single polypeptide chain that contains 583 amino acid residues and 17 intrachain disulfide bridges, forming three domains giving rise to a heart-shaped structure of the protein (Assadpour and Jafari, 2019; Mehmood et al., 2019; Peng, Hidajat and Uddin, 2005; Sigma Aldrich). Additionally, the protein contains two tryptophan, 20 tyrosine and 27 phenylalanine residues (Möller and Denicola, 2002; Peters, 1995).

It has been noted that BSA can return to its normal conformation after being exposed to moderate pH and temperature and due to its many structural advantages, BSA is also essential in drug delivery applications since it can bind to drugs and biochemical compounds that have diverse physicochemical properties (Assadpour and Jafari, 2019; Mehmood et al., 2019).

2.2.4. Lysozyme

Lysozyme is an enzyme with a molecular weight of 14.3 kDa (Sigma Aldrich) and a pI of 11.1 has one single polypeptide chain containing 129 amino acids (Peng, Hidajat and Uddin, 2005; Phillips, 1967). A globular and compact protein with an active site on its surface is formed when the polypeptide is exposed to physiological conditions (Biological Magnetic Resonance Data Bank, 2017). The enzyme is abundant in animals (such as in hens' egg white) and plants as well as in mucosal linings, tears, saliva and nasal secretions. It is known to have an antibacterial activity since it hydrolyses the β-(1→4) glycosidic bond between amino sugars *N*-acetylmuramic acid and *N*-acetylglucosamine in peptidoglycan, the cell wall component of gram positive bacteria (Biological Magnetic Resonance Data Bank, 2017; Prieur, Olson and Young, 1974). Hence, the protein can be used to purify protein and DNA from bacteria (Sigma Aldrich). Furthermore, this single polypeptide chain contains six tryptophan and three tyrosine residues (Formoso and Forster, 1975; Strosberg, Van Hoeck and Kanarek, 1971).

3. Analysis methods

3.1. UV-Vis spectrometry

UV-Vis spectrophotometry is an analytical technique that utilizes radiation in the ultraviolet (UV) and visible (vis) region (～200-800 nm) to induce electronic transitions of analytes in solution or gas phase. The radiation hits the sample and is partly absorbed by the analytes and other interfering substances in the sample. The non-absorbed radiation is measured by a detector and by knowing how much radiation originally was transmitted, the detected signal is converted to an absorbance value. The resulting spectrum, showing absorbance as a function of wavelength, can be used for quantitative and qualitative analysis. The absorbance of the sample follows Beer's law, which means that the absorbance is directly proportional to the concentration of the analyte in the sample. The part of the molecule that is responsible for the absorption is called the chromophore, and this is often an aromatic ring or a conjugated system in the molecule. By altering substituents on the aromatic rings or the conjugated systems, the maximum absorption wavelength of the molecule can be changed. If the tertiary structure of the molecule is changed due to a different environment such that more or less aromatic rings or conjugated systems are exposed, the absorption spectrum for the molecule will also change (Worsfold and Zagatto, 2019).

3.1.1. Uses of derivative spectroscopy

The derivatives (first, second, third order etc.) of the curve for the absorbance as a function of the wavelength (zero-order) can be used for quantitative as well as qualitative analysis of spectra. The even numbered derivatives will have either a peak maximum or minimum at the same wavelength where the zero-order spectrum (absorbance vs wavelength) has its maximum absorbance, whereas the odd numbered derivatives will have a value of zero at this point. If the zero-order spectrum follows Beer's law and shows a linear relationship between the absorbance and the concentration of the analyte, the amplitude of the derivatives will also have a linear proportionality with respect to the concentration. Derivative spectroscopy can increase the accuracy of quantification since it can eliminate baseline shifts, decrease scattering effects as well as discriminate broad absorbance bands resulting from interfering components. In qualitative analysis, derivative spectroscopy can be useful for detection of trace elements in a strongly absorbing matrix. However, the signal-to-noise ratio will be decreased for higher-order derivatives due to the discrimination of broader absorbance bands and the fact that the bands from noise often are the sharpest in the absorbance spectrum (Owen, 2000).

As higher order derivatives are used, the more complex the spectra will become. However, this can be an advantage when comparing two different spectra that are very similar in the zero-order since the higher-order derivatives can reveal the differences that are not as apparent in the absorbance spectra (Owen, 2000). This will facilitate the analysis when comparing two absorbance spectra of the same protein in different environments, to see whether or not the protein has the same spectral features in both spectra and thus be able to conclude if the protein adopts the same conformation in both cases.

3.2. FT-IR spectroscopy (Fourier transform-infrared spectroscopy)

Infrared (IR) spectroscopy is a method used to examine the structure of small molecules and biological systems. Protein folding and unfolding are examples of processes that can be investigated. Some advantages of this technique are that it is applicable for investigation of different types of proteins, such as both soluble proteins and membrane proteins, and it requires low quantities of sample (10-100 μg). Vibrational transitions of molecules are excited when absorbing infrared radiation. Inter- and intramolecular bonds, that affect how strong and polar the vibrating bonds are, will influence the vibrational frequency as well as the probability of absorption. When the polarity is enhanced, the absorption strength will be enhanced. One difficulty with this technique, that can also be considered as an advantage, is that all polar bonds are able to contribute to the IR absorption. This may be beneficial because biomolecules do not need to be labelled since all of them can absorb IR radiation. However, the disadvantage is that these biomolecules give rise to many overlapping bands. The IR-spectrum is constructed by plotting the absorbance against the wavenumber, which is the inverse of the wavelength. The wavenumber, with the unit cm^{-1}, is also proportional to the transition energy. The IR region ranges from 0.78-1000 μm and can be divided into the near-, mid- and far-infrared region, where the near region covers 0.78-2.5 μm and the far-infrared region covers 50-1000 μm (Barth, 2007).

In this investigation, Fourier transform-infrared (FT-IR) spectrometry has been utilized. An FT-IR spectrometer is widely used to obtain an infrared spectrum of absorption, emission, Raman scattering etc. that covers spectral data over a wide range of wavelengths simultaneously. Besides covering a wide spectral range, another advantage is that the sample can be in a liquid, solid or gas phase (Dwivedi et al., 2017). Due to many overlapping bands, it is not possible to extract the chemical structure from molecules using infrared spectroscopy. However, the changes in chemical structure e.g. the protonation states of different side chains in proteins or protein modifications such as phosphorylation can be evaluated by the technique. Furthermore, the amide vibrations are considered as being essential for secondary structure analysis of proteins since the vibrations are highly affected by the secondary structure of the backbone. One example of amide vibrations is the amide I vibration (due to CO-stretching vibrations) that appears at wavenumbers close to 1650 cm^{-1} (Barth, 2007).

3.3. Fluorescence spectroscopy

Molecules possess different states of energy (called energy states) where the lowest energy state is referred to as the ground electronic state and a higher vibrational energy state (when the molecule has absorbed light) is referred to as the excited electronic state. Within these electronic ground and excited states there also exist sub levels (called vibrational levels). When a molecule absorbs energy, it will reach a vibrational level of an excited state and, due to collisions, it will lose the excess energy and drop to the lowest vibrational level of that particular excited state. The majority of molecules will fall from the lowest vibrational level of a higher excited state to a higher vibrational level of a lower excited state. The molecules will then further fall down to the lowest vibrational level of that excited state. Eventually, the molecules will reach their ground electronic state and emit photons with different energies depending on which vibrational level of the electronic ground state the molecules reach. This emitted energy can be used to probe different properties of such molecules. There are three amino acids in proteins that fluoresce and these are tyrosine (Tyr), phenylalanine (Phe) and tryptophan (Trp). Phe has a very low absorptivity and a low quantum yield, while the other two amino acids have a similar quantum yield. Even though Trp and Tyr have similar quantum yields, it has been shown that the indole group of Trp seems to be the dominant source of UV absorption at wavelengths around 280 nm and emission at around 350 nm in proteins (Ghisaidoobe and Chung, 2014; Möller and Denicola, 2006). The environment of the tryptophan chromophore is mainly measured at excitation wavelengths of 290 ±5 nm (Desbois, 2013).

Fluorescence spectra are usually presented as emission spectra where the emission intensity is plotted against wavelength (in nm) or wavenumber (in cm^{-1}). The emission spectra depend on the chemical structure of the fluorescent substance and the interactions with the solvent it is exposed to. The advantage with this technique is the high sensitivity and that a lot of molecular information can be provided (Lakowicz, 2006).

4. Materials and methods

4.1. Materials

Chemicals and proteins that have been used in the project are listed in *Table 1*.

***Table 1**. List of chemicals and proteins, chemical formula, CAS number and supplier of the chemicals and proteins used in the project.*

Name	**Chemical formula**	**CAS number**	**Supplier**
BSA		9048-46-8	Sigma Aldrich
Lysozyme (chicken egg white)		12650-88-3	Sigma Aldrich
Choline chloride	$C_5H_{14}ClNO$	67-48-1	Sigma Aldrich
Choline acetate	$C_7H_{17}NO_3$	14586-35-7	Sigma Aldrich and IoLiTec
Glycerol	$C_3H_8O_3$	56-81-5	Sigma Aldrich
Urea	CH_4N_2O	57-13-6	Sigma Aldrich
Milli-Q water	H_2O		
Sodium phosphate, monobasic, 99%	NaH_2PO_4	7558-80-7	Acros Organics
Sodium hydroxide, 0.1 M	NaOH	1310-73-2	VWR Chemicals

4.2. Methods

4.2.1. Preparation of the DESs and protein samples

The chemicals needed for the DESs were vacuum dried at 70 °C (choline chloride, urea) or 50 °C (choline acetate) for 24 hours before preparation of the DESs. The different DESs (ChCl:Gly, ChCl:U and ChAc:Gly, all in the molar ratio 1:2) were prepared by weighing the required amounts of each chemical into a round bottom flask, followed by continuous stirring (with magnetic bar) and heating at 80 °C for 2-3 hours until a clear deep eutectic solvent was formed. Calculations for the required amount of each chemical to reach the molar ratio 1:2 can be found in *Appendix A*. After cooling, the DESs were equilibrated at room temperature in a desiccator for a minimum of two days before use.

10 mM Phosphate buffer (pH 7) was prepared by adding 1.2 grams of NaH_2PO_4 to a 1 L round bottom flask containing 900 mL of MilliQ-water, equipped with a magnetic bar. NaOH was then added gradually, during stirring, until a pH of 6.99±0.01 was reached. Milli-Q water was finally added to reach a volume of 1 L.

The protein stock solutions were prepared by adding the required amounts of BSA or lysozyme in Milli-Q water to obtain a protein concentration of 1000 µM (*Appendix B*). Each protein solution was then centrifuged at 13 000 rpm for 1 min, followed by pipetting of the supernatant into new tubes. Dilution (2x and 10x respectively) of the 1000 µM samples were conducted to obtain the lower concentrations of 500 and 100 µM. Centrifugation and pipetting of the supernatant into new tubes were also conducted for each of the lower concentrations after dilution. Protein solutions in phosphate buffer were prepared in the same manner as for the protein in Milli-Q. Final concentrations of protein in buffer were however 100, 50 and 10 µM compared to 1000, 500 and 100 µM in Milli-Q. Both protein stock solutions and protein in buffer were stored at 4 °C between the measurements and were used for the experiments within one week to avoid degradation of the proteins.

Protein in DESs-samples with protein concentrations of 100, 50 and 10 μM were prepared by mixing the required amount of DES and protein stock solution in a glass tube/bottle. The added amount of protein stock solution was always 10x lower than the added amount of DES, to reach a final protein concentration that was 10x lower than in the protein stock solution. All samples were then freeze dried for 24 hours for removal of the water, resulting in a homogenous DES with incorporated protein. Samples were at all times stored at 4 °C when not used for measurements.

Hydrated ChCl:Gly with 2, 5, 10, 20 and 50 wt% water, containing protein with a concentration of 50 μM, as well as hydrated ChCl:Gly with 2, 5, 10, 20 and 56 wt% water containing protein with a concentration of 10 μM were prepared by mixing the required amounts of pure DES, protein solution and Milli-Q water. Added amounts can be found in *Appendix C*. The hydrated DESs-samples were then stored at 4 °C for 24 hours before measurements for equilibration. Samples were at all times stored at 4 °C when not used for measurements.

Dialysis of the proteins (extraction of protein from DES to buffer) was performed with a Spectra/Por® 7 Dialysis Membrane (Pretreated RC Tubing, MWCO: 8 kD). ChCl:Gly with BSA or Lys in the concentrations of 50 and 100 μM were used for the extractions, and these were extracted to phosphate buffer after 40 days in ChCl:Gly. Each sample was pipetted into a separate membrane tube, sealed with clips and put in a beaker containing phosphate buffer and equipped with a magnetic bar. The beaker was continuously stirred for 2-3 hours before the phosphate buffer was exchanged with fresh buffer. Three dialysis cycles were performed for each sample, where the third cycle took place overnight at 4°C (without stirrer) in order to prevent degradation of protein.

4.2.2. Experimental setup

Determination of BSA and lysozyme concentrations was conducted using a ND-1000 Spectrophotometer (Saveen Werner). The absorbance was measured at 280 nm, and the concentrations in mg/mL were obtained directly from the software. Extinction coefficients for BSA and lysozyme are 43 824 and 38 940 cm^{-1} M^{-1}, respectively, and the molecular weights are 66 400 and 14 300 g/mol, respectively.

UV-Vis measurements were performed using the Varian Cary 50 UV-Vis Spectrometer. A quartz cell with a light path of 1 mm, as well as a spacer, both from Hellma Analytics, were used. The absorbance was measured in the range 190-500 nm with a medium scan speed (600 nm/min), dual beam mode and baseline correction.

FT-IR measurements were performed using the Nicolet 6700 FT-IR with ATR mode, a diamond crystal and a DTGS KBr detector. A number of 64 scans were performed for each measurement (background collection performed with 512 scans) with a resolution of 4 cm^{-1}. The absorbance was measured in the range 400 to 4000 cm^{-1} after the undiluted sample had been put on the diamond crystal. ATR correction with a number of bounces of 1.0 was used.

Fluorescence measurements were performed using the Cary Eclipse Fluorescence Spectrometer in the 96 Wells plate configuration. Measurements were conducted at excitation wavelengths of either 280 or 295 nm, with a number of 15 scans for each measurement. Emission intensity was measured in the range 285-600 nm and 300-600 nm for each excitation wavelength, respectively, with an excitation and emission slit of 5 nm and medium scan speed (rate: 600 nm/min).

5. Results and discussion

5.1. NanoDrop measurements

NanoDrop measurements were used to confirm that the right amount of protein had been introduced to the samples. For the stock solutions (BSA and lysozyme in water), NanoDrop measurements showed that the concentration of protein in the samples were approximately the same as the calculated concentration, except that BSA had a slightly lower concentration than expected (e.g. $[BSA100]_{real}$= 56 mg/mL vs $[BSA100]_{calc}$= 67 mg/mL). For the proteins in phosphate buffer, obtained values corresponded to added concentrations.

For the proteins in ChCl:Gly, the obtained concentrations from the NanoDrop were consistent with the added concentrations. For the proteins in ChCl:U, the concentration of lysozyme obtained from the measurements was consistent with added concentration. For BSA, the 100 μM sample had too many aggregates to be able to make reliable measurements and the 50 μM sample showed concentration values that were slightly higher than added concentrations. No reliable concentration values were obtained for both of the proteins in ChAc:Gly and this may be due to sample degradation as these showed a yellow appearance (see Discussion for further details).

The values obtained from the measurements of hydrated ChCl:Gly samples showed somewhat higher concentrations than theoretically calculated concentrations. The explanation for this is that weight was used instead of volume when adding the amount of ChCl:Gly to the samples. The density of ChCl:Gly is slightly larger than 1 g/mL, resulting in that 5 g of total sample is not corresponding to a volume of 5 mL (which was used for calculations) but instead a slightly smaller volume. The protein was therefore added to a smaller volume than calculated, resulting in a slightly higher concentration than expected. Weight was used instead of volume when adding ChCl:Gly since the DES was viscous, making it hard to pipette the right amount needed.

The dialyzed proteins were extracted to a bigger volume of buffer (e.g. 5 mL samples of protein in DES were extracted to 2-3 times bigger volume of buffer), resulting in dilution of original protein concentration. This was confirmed by the NanoDrop measurements.

5.2. Neat DESs: UV-Vis measurements

The concentrations for BSA and lysozyme that were used for the UV-Vis measurements were 10, 50 and 100 μM. However, due to obtaining low absorbance (below 0.05) for both proteins in the concentration of 10 μM, only data for proteins in the concentrations of 50 and 100 μM were further investigated. In *Figure 1, 2 and 3* it can be seen that the absorbance of the proteins in the DESs are rather similar to the respective concentrations in aqueous buffer except for BSA in ChCl:U (see discussion below). This indicates that little protein was lost when proteins were incorporated into the different DESs. The figures also depict that the absorbance increases with increasing concentration, which is expected since the UV-Vis signal is directly proportional to the total amount of protein present.

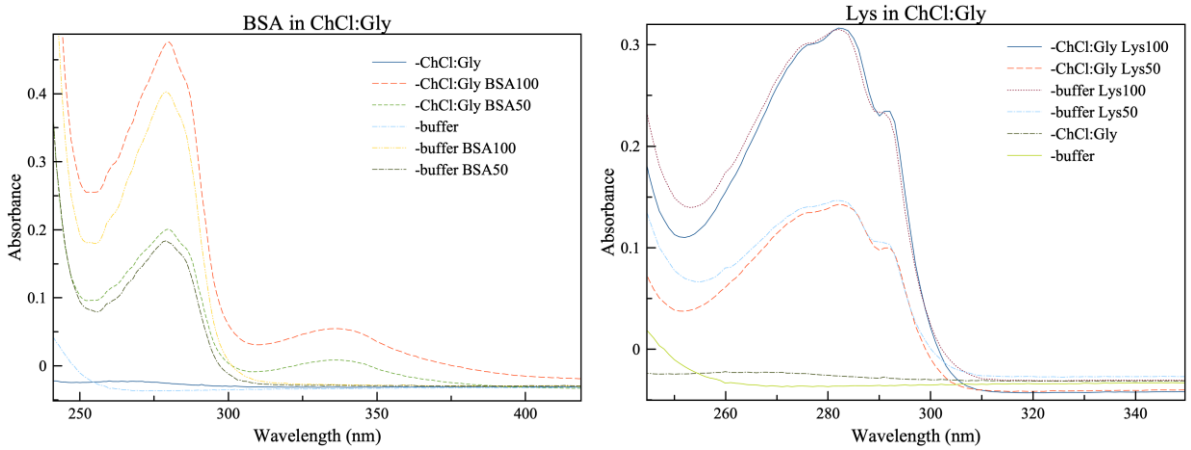

Figure 1. *Absorbance curves of BSA (left) and Lys (right) in ChCl:Gly and buffer. Data for proteins (50 and 100 μM) in buffer and ChCl:Gly are shown, as well as absorbance curves of pure buffer and pure ChCl:Gly.*

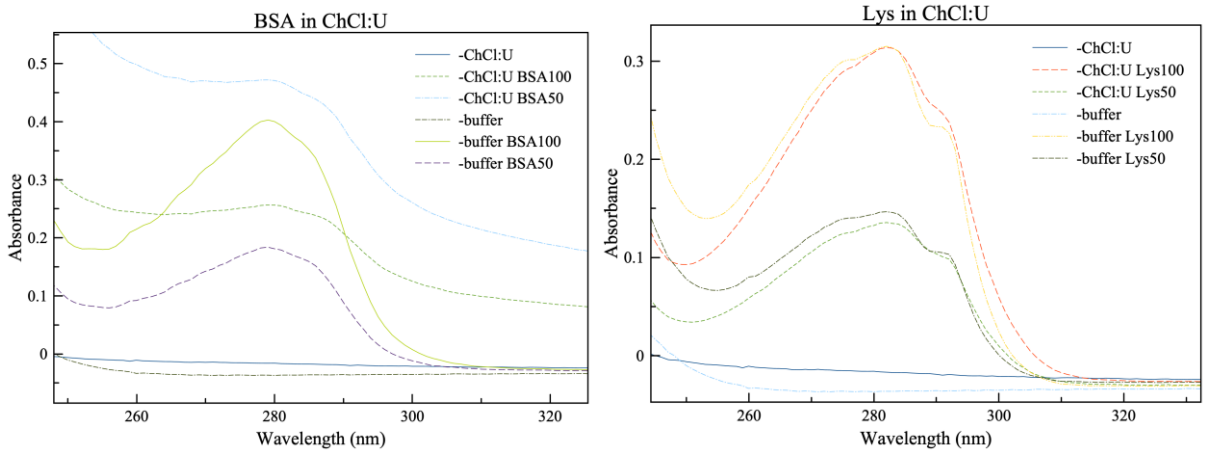

Figure 2. *Absorbance curves of BSA (left) and Lys (right) in ChCl:U and buffer. Data for proteins (50 and 100 μM) in buffer and ChCl:U are shown, as well as absorbance curves of pure buffer and pure ChCl:U.*

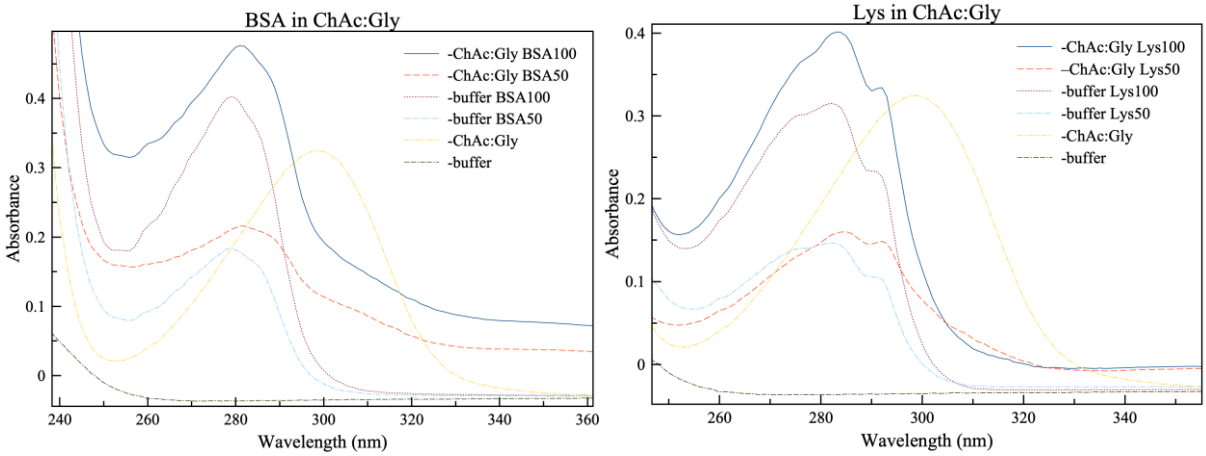

Figure 3. *Absorbance curves of BSA (left) and Lys (right) in ChAc:Gly and buffer. Data for proteins (50 and 100 μM) in buffer and ChAc:Gly are shown, as well as absorbance curves of pure buffer and pure ChAc:Gly.*

5.2.1. ChCl:Gly

The absorbance curves of BSA in ChCl:Gly are similar to the curves of BSA in buffer between 240 and 300 nm wavelengths *(Figure 1)*, which indicates that the protein conformation is mostly retained when BSA is in ChCl:Gly (In *Appendix D*, normalized curves of each graph are depicted, which makes it easier for comparison of shapes). Furthermore, an additional peak is apparent in the wavelength range 300-400 nm for BSA in ChCl:Gly. A possible reason for this is that interactions have occurred between BSA and ChCl:Gly or the separate components, giving rise to the peak.

In *Figure 1* it can be seen that the overall shape of the curve of lysozyme in ChCl:Gly show some small differences compared to the shape of the curve for lysozyme in buffer. This may indicate that a slightly different conformation of Lys is present in ChCl:Gly.

5.2.2. ChCl:U

The curve of BSA in ChCl:U (*Figure 2*) shows a sloping baseline. The reason for this as well as the deviating concentrations of BSA in ChCl:U, can be that the samples were very turbid and contained aggregates after the freeze drying process. This suggests that aggregation of BSA has occurred in the freeze drier due to exposure to harmful conditions such as bubbling. The graph for BSA in ChCl:U also displays that the curve of BSA in ChCl:U and buffer are not similar to each other. This could either be due to a changed conformation of BSA in ChCl:U, sample degradation or aggregates being present.

Just as for BSA in ChCl:U, the curves of lysozyme in ChCl:U (*Figure 2*) differ from the curve of lysozyme in buffer, also indicating a possible change in conformation of lysozyme in ChCl:U.

5.2.3. ChAc:Gly

Interestingly, pure ChAc:Gly gave an absorbance peak at the wavelength range 260-340 nm, which was unexpected. Nothing regarding this was found in literature and when measuring pure choline acetate and pure glycerol (the components of ChAc:Gly), no absorbance peak was found at these wavelengths. Therefore, baseline subtraction was conducted for the absorbance curves of protein in ChAc:Gly before interpretations were made.

BSA in ChAc:Gly (*Figure 3*) gives rise to a sloping baseline, which can be due to the distinct yellow color of the samples after freeze drying. A possible explanation for the yellow color is the lack of control of the conditions (which make it difficult to keep the samples frozen during the whole process) in the freeze dryer used, causing unwanted changes of the samples. It is also known that BSA dissolved in water causes a slight yellow color of the solution (from Sigma Aldrich product information). The sloping baseline did not appear for lysozyme in ChAc:Gly, but the samples were likewise somewhat yellow (though to a smaller extent). Nevertheless, it can be seen that the peak for BSA in ChAc:Gly is broader compared to the peak for BSA in buffer. The curve of lysozyme in ChAc:Gly also shows that a slight change has occurred compared to the curve of lysozyme in buffer. Moreover, a slight shift of λ_{max} has occurred towards longer wavelengths for both proteins in ChAc:Gly compared to when they are in buffer. All this suggests that both BSA and lysozyme adopts different conformations in ChAc:Gly.

5.2.4. Comparison of BSA and lysozyme in all three DESs and buffer

When comparing BSA and lysozyme in all of the DESs and buffer (*Figure 4*), the protein concentration 50 µM was chosen as the most suitable for comparison. This because 10 µM gave too low absorbance and BSA in ChCl:U and ChAc:Gly in the concentration 100 µM led to aggregation or a distinct yellow sample. *Figure 4* presents absorbance curves for both proteins in all three DESs; ChCl:Gly, ChCl:U and ChAcGly, as well as in phosphate buffer. From the graphs it can be observed that the absorbance of BSA in ChCl:U is higher than the absorbance of BSA in the other DESs and buffer. An explanation to this observation can be that the aggregates of the sample led to a different signal that resulted in more strongly absorbing protein, but the origin of this difference is still unclear. When considering the shapes of the curves, it is evident that the curves of BSA in the different DESs are not similar to each other, with the curve of BSA in ChCl:Gly being the most similar to the curve of BSA in buffer (see *Appendix D* for normalized graphs and easier visualization of similarities/differences between the curves). This suggests that the native conformation of BSA is best retained in ChCl:Gly compared to ChCl:U and ChAc:Gly. However, BSA in ChCl:U had more aggregates and BSA in ChAc:Gly resulted in yellow samples, which might have affected the measurements.

The absorbance curves of lysozyme in all of the three DESs and buffer *(Figure 4)* depict that lysozyme retains a similar shape in ChCl:Gly and ChCl:U compared to buffer (where the biggest difference is seen at the wavelength 290 nm), with the biggest similarity between lysozyme in ChCl:Gly and buffer. The absorbance curve of lysozyme in ChAc:Gly is the curve that differs the most compared to the buffer and the two other DESs, suggesting that the protein has changed its native conformation in ChAc:Gly. However, the samples turned yellow during the sample preparation and thus might have affected the measurements in the UV-Vis spectrometer.

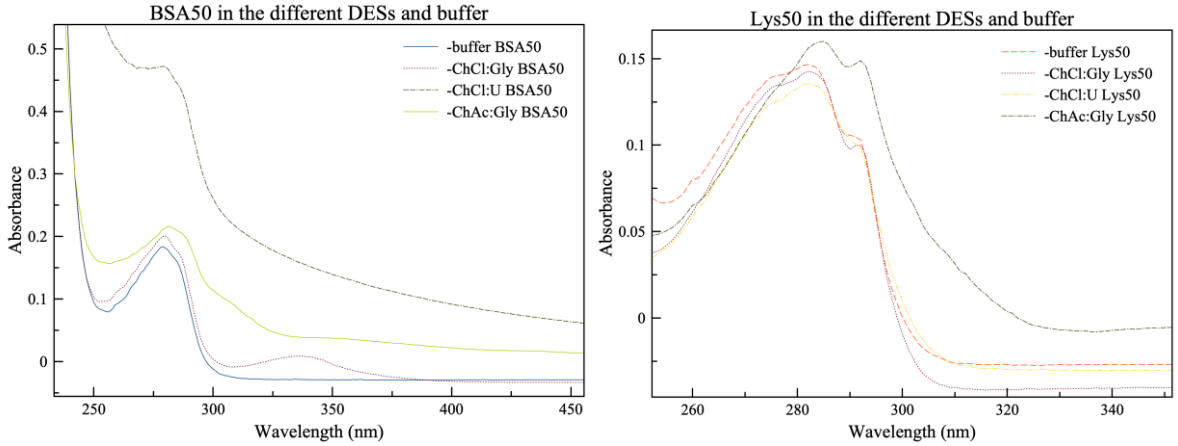

Figure 4*. Comparison of BSA (left) and lysozyme (right) in the three different DESs and buffer. Data for both BSA and lysozyme in the concentration of 50 µM in the different DESs and buffer can be seen.*

5.3. Neat DESs: FT-IR measurements

The concentrations of BSA and lysozyme measured in the FT-IR were 10, 50 and 100 µM. However, due to weak signal of both proteins in the concentrations of 10 µM and 50 µM, only data for proteins in the concentration 100 µM was further investigated. For both proteins in all of the three DESs and buffer, the amide I peak of the pure proteins was not seen or only existent to a small extent when the proteins were in the DESs or buffer (*Figure 5, 6, 7 and 8*). A possible explanation for this might be that the concentration of protein was too low for showing this experimental feature. Nevertheless, a common result for both BSA and lysozyme in the different DESs is that all other significant peaks for each individual protein are lost when the proteins are in the different DESs.

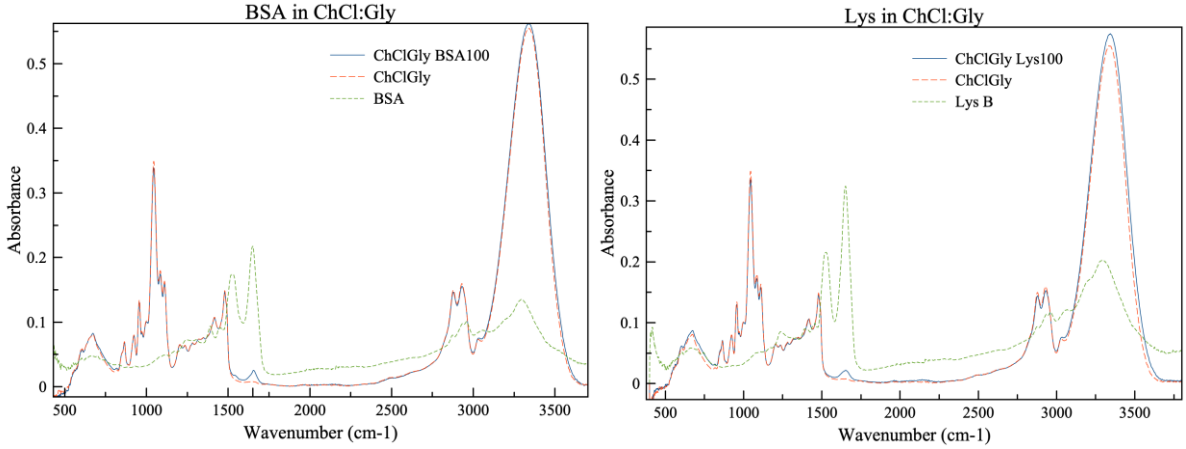

***Figure 5**. Graph of BSA (left) and lysozyme (right), both in the concentration 100 µM, in ChCl:Gly. In respective graph, curves of the pure proteins, pure ChCl:Gly and protein in ChCl:Gly are shown. The amide I peak of the proteins can be detected at an approximate wavenumber of 1650 cm^{-1}.*

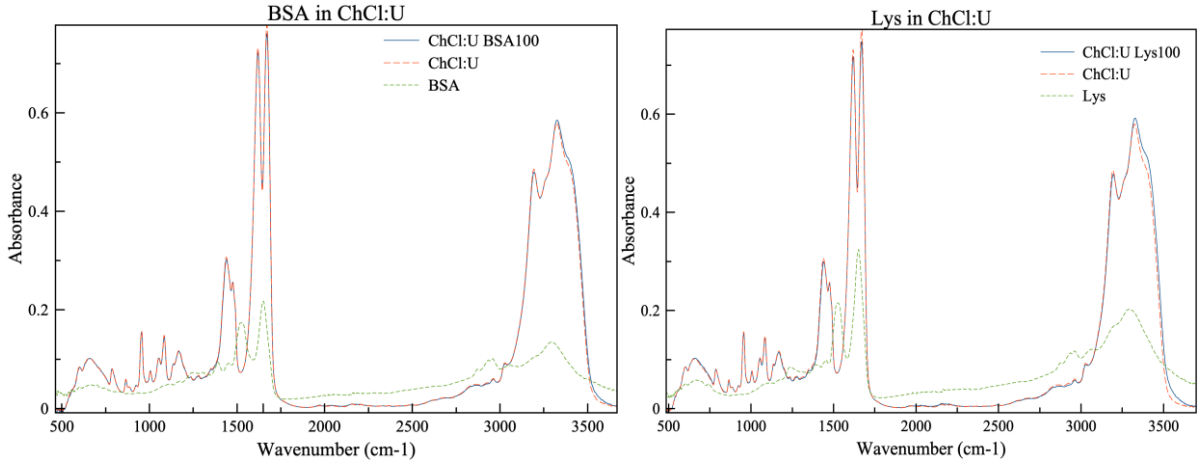

***Figure 6**. Graph of BSA (left) and lysozyme (right), both in the concentration 100 µM, in ChCl:U. In respective graph, curves of the pure proteins, pure ChCl:U and protein in ChCl:U are shown. The amide I peak of the proteins, that can be detected at an approximate wavenumber of 1650 cm^{-1}, are hidden behind a peak of ChCl:U when the proteins are in the DES.*

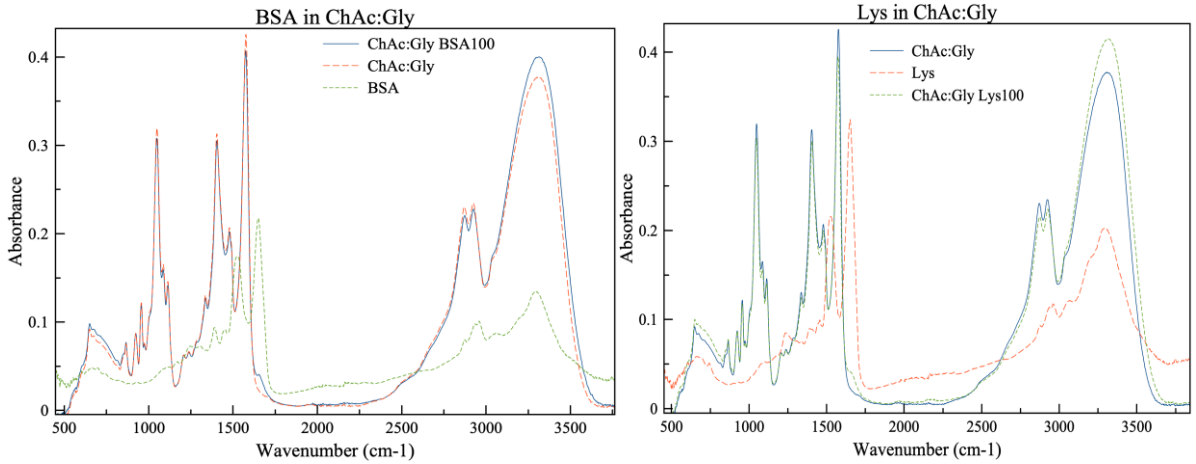

***Figure 7**. Graph of BSA (left) and lysozyme (right), both in the concentration 100 µM, in ChAc:Gly. In respective graph, curves of the pure proteins, pure ChAc:Gly and protein in ChAc:Gly are shown. The amide I peak of the proteins, that can be detected at an approximate wavenumber of 1650 cm^{-1}, are only existent to a small extent when the proteins are in ChAc:Gly because the DES has a large peak in this region.*

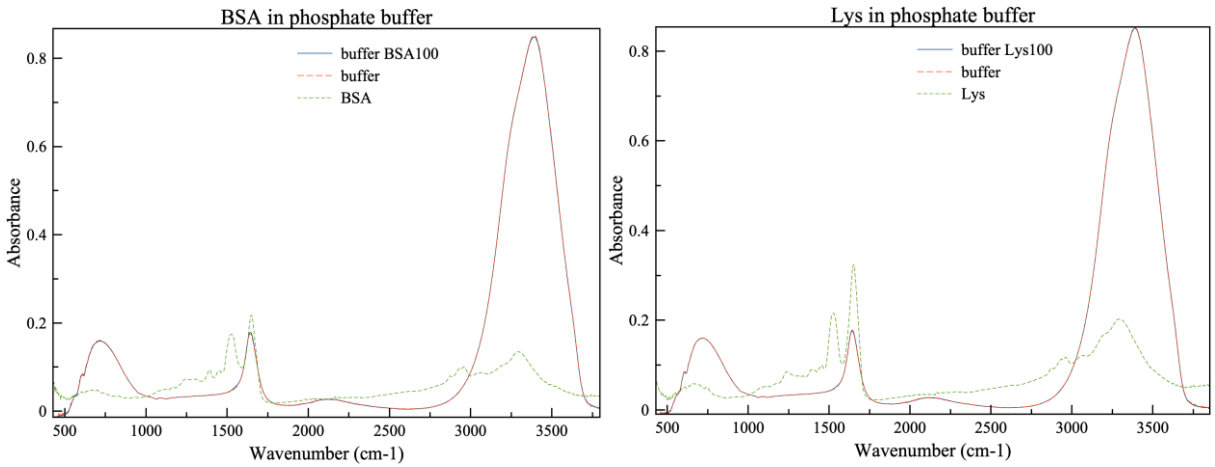

***Figure 8**. Graph of BSA (left) and lysozyme (right), both in the concentration 100 µM, in buffer. In respective graph, curves of the pure proteins, pure buffer and protein in buffer are shown. The amide I peak of the proteins in buffer, that can be detected at an approximate wavenumber of 1650 cm^{-1}, are hidden behind a large peak of the buffer.*

In the graph for BSA in ChCl:Gly (*Figure 5*), it can be seen that pure BSA has a relatively high absorbance (approximately 0.2) at wavenumber 1650 cm^{-1}, emerging from the amide I bond. However, the amide I peak decreases significantly for BSA in ChCl:Gly, giving an absorbance of approximately 0.03. This suggests that the protein is present, but in a low concentration. When comparing the curves for pure lysozyme, pure ChCl:Gly and lysozyme in ChCl:Gly (*Figure 5*), the same observation can be made.

The amide I peak of both BSA and lysozyme in ChCl:U has been hidden behind a peak originating from ChCl:U (*Figure 6*). Furthermore, the amide I peak of the proteins is very weak when the proteins are in ChAc:Gly (*Figure 7*) and this is because ChAc:Gly has a dominating peak that starts at that position and hence hides the peak of interest.

The graphs for BSA and lysozyme in phosphate buffer are displayed in *Figure 8*. The peaks originating from the proteins are hidden behind the buffer, which shows a larger peak where the amide I peak normally emerges. No other peaks belonging to the pure proteins are observed when the protein is exposed to the buffer. These observations are however expected due to the fact that the buffer contains water, which gives a strong signal in the FT-IR, especially in the amide I region. Hence, compounds that are normally recognized with the FT-IR can often become undetected when being exposed to water (Gasdia-Cochrane, 2018).

The absorbance of protein in DESs and buffer needed to be subtracted with the absorbance for pure DESs and buffer to be able to analyze the shapes of the absorbance curves. The resulting curves were further normalized to the amide I peak *(Figure 9)* for easier analysis of this peak, which allows changes in the secondary structures to be observed. As stated above, neither BSA or lysozyme exhibited a peak in the amide I region when the proteins were in ChCl:U and therefore these curves were not considered when normalizing the graphs below.

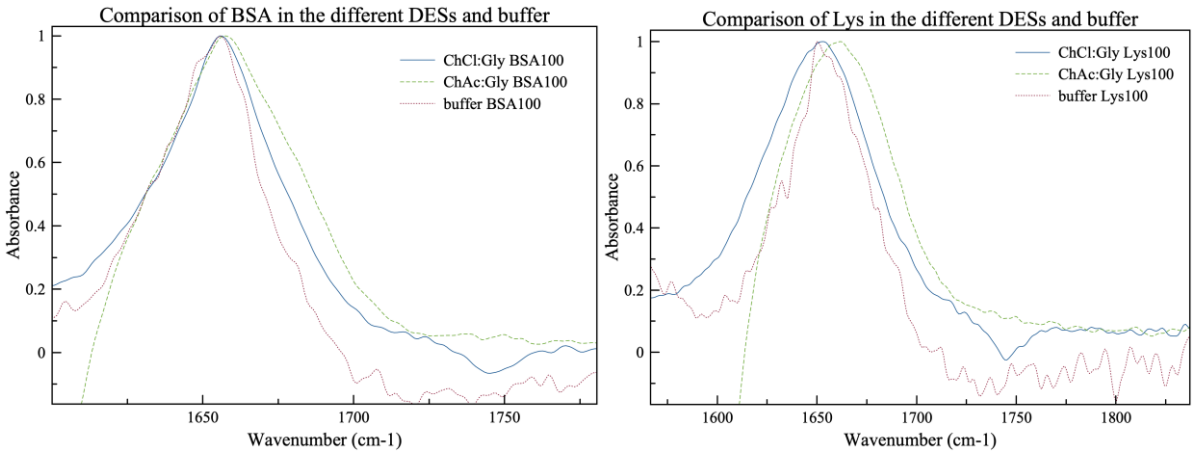

***Figure 9**. Normalized FT-IR absorbance curves of BSA (right) and lysozyme (left), both in the concentration 100 µM, in the different DESs and buffer (after subtraction with respective pure DES or phosphate buffer). A zoom of the amide I peak has been made for easier comparison of the shapes. The curves of the proteins in ChCl:U are omitted since the amide I peak of the proteins in this DES could not be seen.*

As can be seen in *Figure 9*, the shapes of the amide I peak has changed for both proteins when they are in ChCl:Gly and ChAc:Gly. The peaks are broader compared to the amide I peak of the proteins in buffer. The change indicates that the secondary structure of the proteins has been altered when they are exposed to the DESs. If there was more time, Gaussian peaks could have been fitted in the amide I peak to be able to evaluate how the secondary structure has been variated.

5.4. Neat DESs: Fluorescence measurements

The concentrations of BSA and lysozyme used for the fluorescence measurements were 10, 50 and 100 µM. No apparent pattern is seen for the intensities between the different concentrations of BSA and lysozyme when they are in the different DESs and buffer *(Appendix E)*. One reason for this can be that a 96-well plate was utilized for the measurements and this plate requires the same height of each sample in order to perform adequate measurements of the emission intensities. Therefore, either the pipetting volumes led to inconsistent heights of the samples or too much protein of the samples with higher protein concentrations led to quenching effects (lower emission intensity due to absorbance of the emitted light of molecules or the solvent), resulting in the different intensities seen (Sen and Dasgupta, 2004). Another interesting observation is that the pure phosphate buffer had an abnormally high emission peak at 320 nm (around 35 emission intensity units), *Appendix E*. This peak was present for three different phosphate buffers (prepared by three different analysts) and a possible explanation of this peak could not be given.

When comparing the emission intensities of the different BSA concentrations in ChCl:Gly, it can be seen that BSA10 gives rise to a pronounced higher emission intensity compared to BSA50 and BSA100 *(Appendix E)*. This might be due to quenching effects, which arises from too much protein being present in BSA50 and BSA100. Moreover, an additional peak at longer wavelengths is seen for BSA50 and BSA100 compared to BSA10. A probable explanation to this is that the excess protein in the samples with higher protein content absorb emitted fluorescence and re-emit this energy at longer wavelengths.

Both lysozyme and BSA in ChAc:Gly showed unexpected emission curves with very low emission intensities. Due to the low intensities and therefore high noise, no valid interpretations could be made regarding the proteins in ChAc:Gly. It remains unclear why the intensities for the proteins in ChAc:Gly were depressed, but one suggestion is that these samples (particularly the BSA samples) had a distinct yellow color that appeared during sample preparation. Another explanation can be that the proteins are clustered in the DES, resulting in little protein actually being present in the sample volume that was transferred to the 96-well plate.

When observing the shapes of the normalized emission spectra for BSA in the different DESs and buffer (*Figure 10, 11 and 12*), it can be seen that the curves for BSA in all of the DESs (except BSA10 in ChAc:Gly) have a shift of λ_{max} towards shorter wavelengths compared to BSA in buffer. A shift of λ_{max} is an indication of a change in the protein conformation or that the protein interactions with the environment has been altered. This occurs when exciting at both excitation wavelengths of 280 and 295 nm. The shift of λ_{max} towards shorter wavelengths indicates that the local environment of the fluorophores has changed to a more hydrophobic one, resulting in a more compact structure of the protein. The shift of λ_{max} at excitation wavelength 295 nm indicates that it is the local environment of Trp residues that has changed (Lakowicz, 2006).

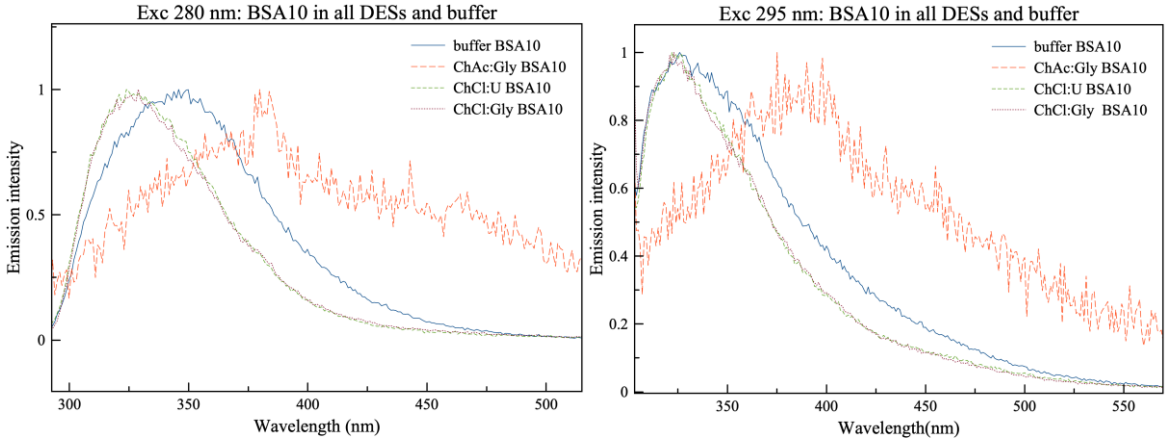

Figure 10. *Normalized emission curves of BSA10 in all DESs and buffer at exc 280 nm (left) and 295 nm (right).*

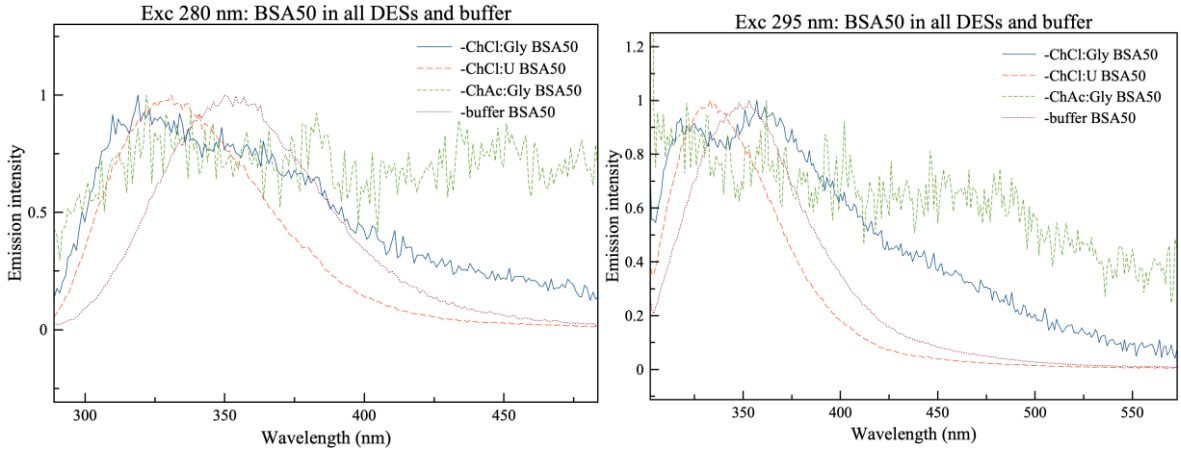

Figure 11. *Normalized emission curves of BSA50 in all DESs and buffer at exc 280 nm (left) and 295 nm (right).*

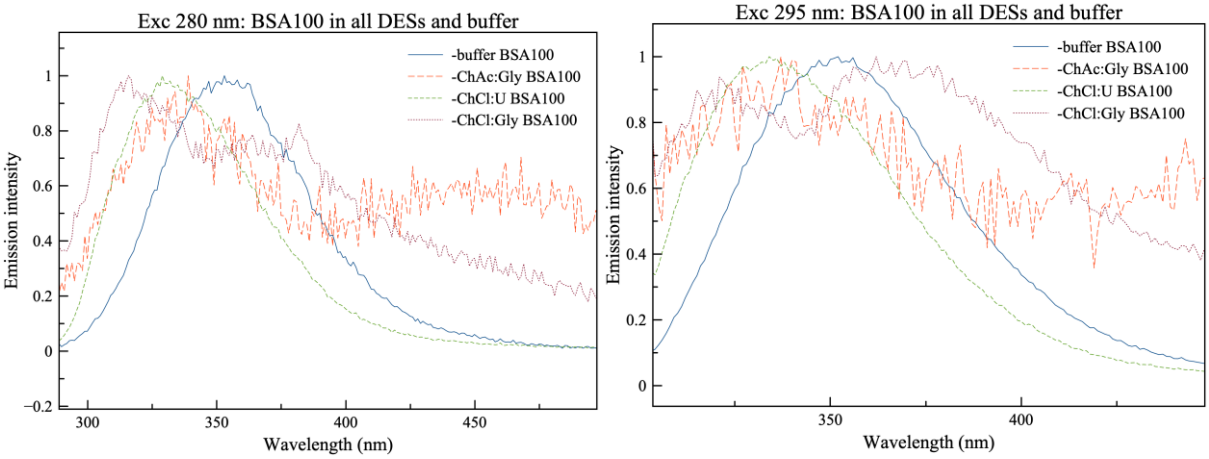

Figure 12. *Normalized emission curves of BSA100 in all DESs and buffer at exc 280 nm (left) and 295 nm (right).*

Analyzing the shapes of the emission spectra for Lys10 in the different DESs and buffer (*Figure 13*), it can be seen that the curves for Lys10 in all of the three DESs have a shift of λ_{max} towards longer wavelengths compared to Lys10 in buffer. This suggests a change in conformation of lysozyme (Lakowicz, 2006). However, this is not seen for Lys50 and Lys100 (*Figure 14 and 15)*, where the shift of λ_{max} to longer wavelengths is not observed.

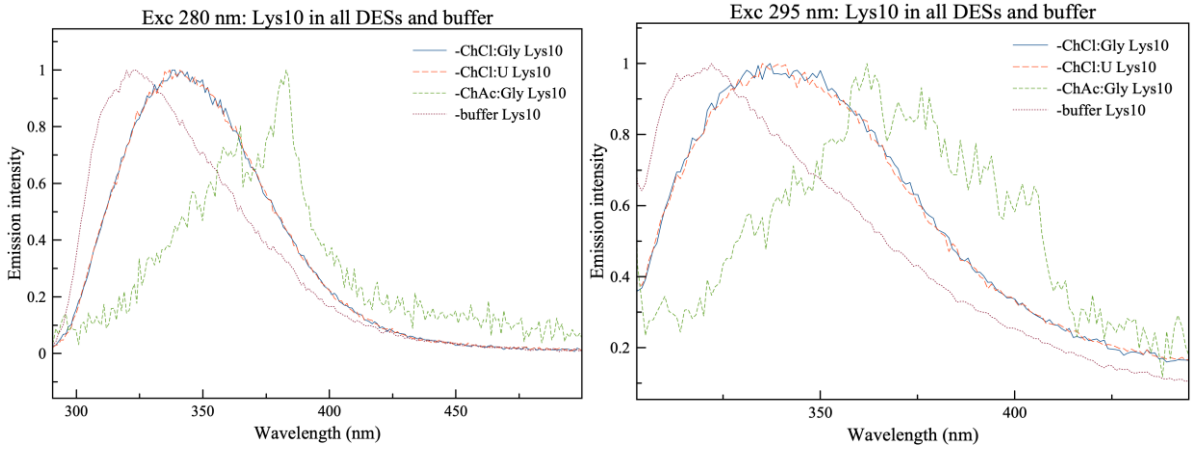

Figure 13. *Normalized emission curves of Lys10 in all DESs and buffer at exc 280 nm (left) and 295 nm (right).*

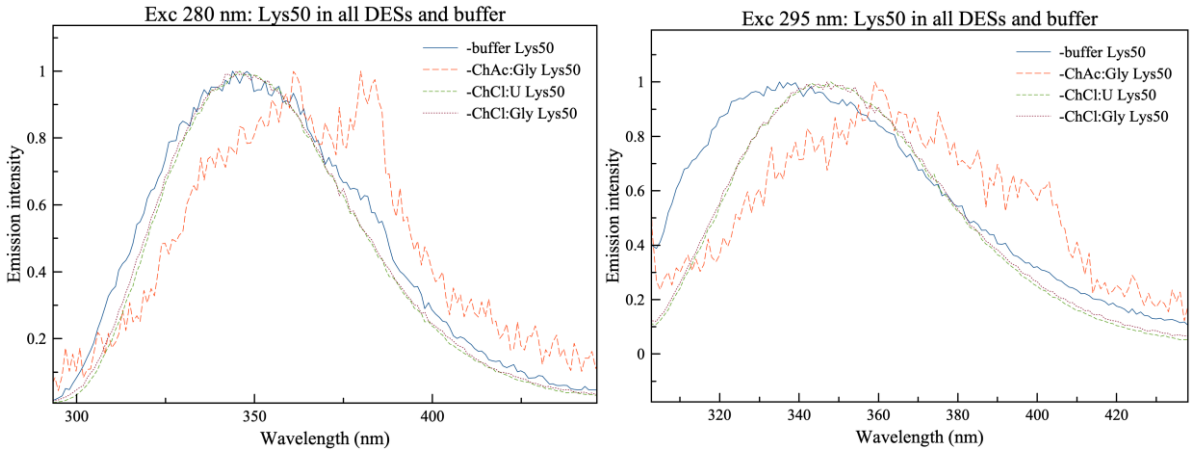

Figure 14. *Normalized emission curves of Lys50 in all DESs and buffer at exc 280 nm (left) and 295 nm (right).*

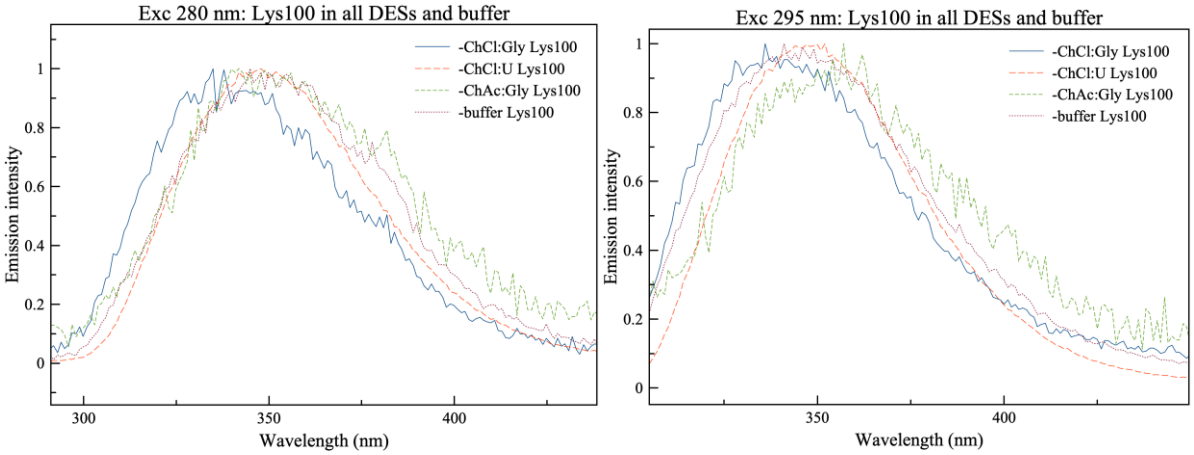

Figure 15. *Normalized emission curves of Lys100 in all DESs and buffer at exc 280 nm (left) and 295 nm (right).*

The findings regarding the shift of λ_{max} described above are generally implemented for proteins in aqueous solutions and it is not known if the same can be said for proteins in DESs that are not aqueous. Therefore, another explanation for the shifts is the various solvent characteristics that cause different interactions between the proteins and the DESs (compared to protein and buffer). The shift of λ_{max} towards shorter wavelengths for BSA and towards longer wavelengths for lysozyme can be due to the proteins having different charges and pI, resulting in different interacting mechanisms with the solvent. Using fluorescence measurements by itself is not enough to conclude if the tertiary structure really has changed since the fluorescence measurements only provide information about the local environment of the fluorophores (Royer, 2006).

5.5. Hydrated DES

As mentioned under 4.2. Methods, hydrated ChCl:Gly with 2, 5, 10, 20 and 50 wt% water (56 wt% water for samples with the protein concentration of 10 µM) with BSA or lysozyme of 50 µM were prepared. The reason why the samples with a protein concentration of 10 µM have a water content of 56 wt% and not 50 wt% water is miscalculations when preparing the samples. HD ChCl:Gly samples with a protein concentration of 10 µM were only used for analyzing fluorescence data, since 50 µM might give rise to quenching effects (as discussed in section 5.4). A protein concentration of 50 µM was used for UV-Vis data and FT-IR measurements.

5.5.1. HD DES: UV-Vis measurements

When comparing the data of the two proteins in HD ChCl:Gly with different water contents (*Figure 16*), somewhat similar absorbance was seen for all solvents. This is expected since all of the samples contained a calculated protein concentration of 50 µM, but in reality had slightly different concentrations due to the use of weight and not volume when adding ChCl:Gly to the hydrated samples (see explanation in section 5.1.). The curves of BSA in HD ChCl:Gly are very similar to the curve of BSA in buffer, which suggests that the protein conformation is more retained when water is added to ChCl:Gly. This observation is supported by a previous study that reported the protein conformation of BSA and lysozyme in pure and hydrated DESs using circular dichroism (CD) and small-angle neutron scattering (SANS), indicating that proteins can attain a more natural conformation when proteins in DES are exposed to water (Sanchez-Fernandez et al., 2017). However, the graph obtained for lysozyme shows conflicting results, where lysozyme in the hydrated samples more resemble lysozyme in pure ChCl:Gly. Another interesting observation for BSA is that the additional peak at 300-400 nm for BSA in pure ChCl:Gly is suppressed when BSA is in HD ChCl:Gly. This peak is even depressed for BSA in HD ChCl:Gly with 2 wt% water, which only contains a small amount of water. For HD ChCl:Gly, the added water is most likely situated around the protein, offering an environment to the protein similar to phosphate buffer. This is possible by the extensive hydrogen bond network formed between the DES components, making it hard for the added water to interact with these (Sanzches-Fernandez et al., 2017; Esquembre et al., 2013).

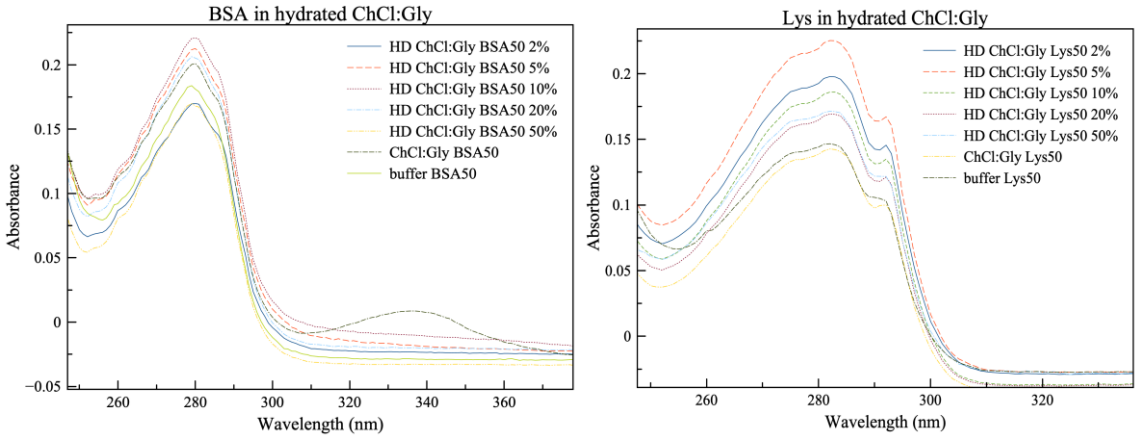

Figure 16. *UV-Vis spectra of BSA (left) and lysozyme (right), both in the concentration 50 µM, in HD ChCl:Gly with different wt% water, pure ChCl:Gly and buffer.*

5.5.2. HD DES: FT-IR measurements

For the FT-IR measurements, it can be observed that the amide I peak increases with increasing water content for both proteins (*Figure 17*). The explanation for this is that the H-O-H vibrations from the water molecules are apparent at the same wavenumbers as the amide I peak. No samples of hydrated ChCl:Gly with corresponding water concentration and without the protein were made and therefore no buffer subtraction could be performed. Hence, comparison of the amide I peak between the different samples had to be made directly (without subtraction) and this is rather difficult since small changes are hard to observe. No conclusions could therefore be drawn about the shape of the amide I peak.

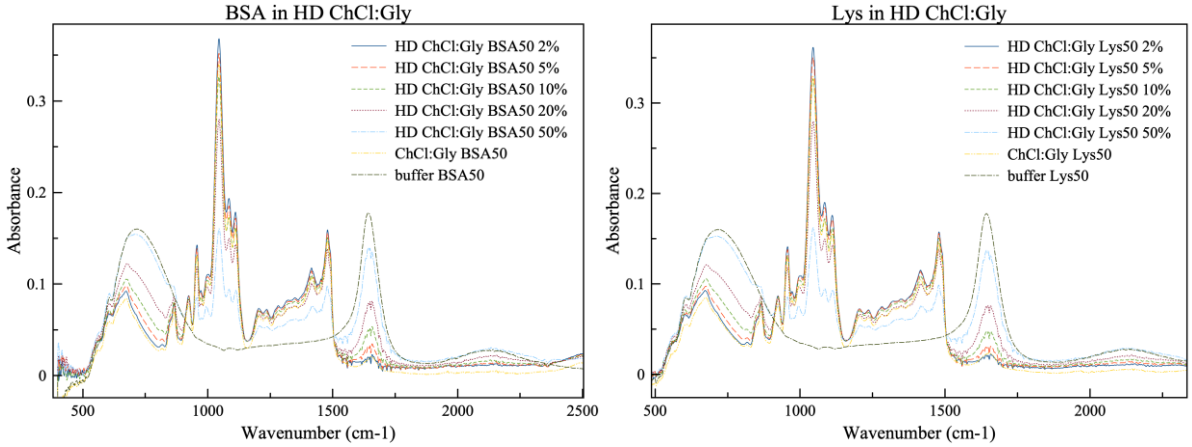

Figure 17*. FT-IR spectra of BSA (left) and lysozyme (right), both in the concentration 50 µM, in HD ChCl:Gly with different wt% water, pure ChCl:Gly and buffer. The amide I peak can be seen in the wavenumber 1650 cm^{-1}.*

Comparison of the overall shapes of the curves shows that the spectra of proteins in HD ChCl:Gly with 50 wt% water are more similar to the spectra of protein in buffer than to the spectra of protein in pure ChCl:Gly. This indicates that the proteins are more in an aqueous environment compared to systems with lower water content (these samples are more of an aqueous solution of the components than a ChCl:Gly DES). In literature it can be found that more similarities regarding the tertiary structure are seen between protein in buffer and protein in hydrated ChCl:Gly compared to the protein in pure DES (Sanchez-Fernandez et al., 2017), supporting the obtained data. Moreover, it can be observed that the shape of the curves changes gradually with increasing water content, where an increasing amount of water in the HD DES prompts more similar features to those in aqueous buffer.

5.5.3. HD DES: Fluorescence measurements

No valid comparisons between the emission intensities for the proteins in HD ChCl:Gly, proteins in pure ChCl:Gly and proteins in buffer can be made since no distinct pattern for the emission intensities has been obtained. Probable explanations affecting the outcome of the emission spectra, such as the heights of the samples in the 96-well plate and quenching effects, have been discussed in section 5.4.

When comparing the normalized curves of BSA in HD ChCl:Gly, pure DES and buffer (at excitation wavelength 280 nm), *Figure 18*, it can be seen that the curves of BSA in HD ChCl:Gly with water contents up to 20 wt% water resemble the curve of BSA in pure ChCl:Gly. It is also seen that the curve of BSA in HD ChCl:Gly with 56 wt% water is similar to the curve of BSA in buffer. This observation is consistent with the data obtained from the FT-IR, where it was seen that HD ChCl:Gly with 50 wt% water was more of an aqueous solution of the DES components. Additionally, λ_{max} of this sample (BSA in HD ChCl:Gly with 56 wt% water) appears at longer wavelengths (more towards BSA in buffer) compared to the other samples, implying that the environment of BSA in these samples is more polar. The normalized spectra of BSA in HD ChCl:Gly in all water concentrations obtained for measurements performed at excitation wavelength 295 nm *(Figure 18)* display similar curves and that the similarity is bigger between BSA in HD ChCl:Gly and BSA in buffer compared to BSA in pure ChCl:Gly. This implies that the local environment of Trp residues is similar when BSA is in buffer and HD ChCl:Gly. This is in agreement with the observation from the UV-Vis measurements of BSA in HD ChClGly (see section 5.5.1), where a peak exhibited by BSA in pure ChCl:Gly was depressed when water was added to the DES, indicating that the water altered the interactions of BSA with the surroundings.

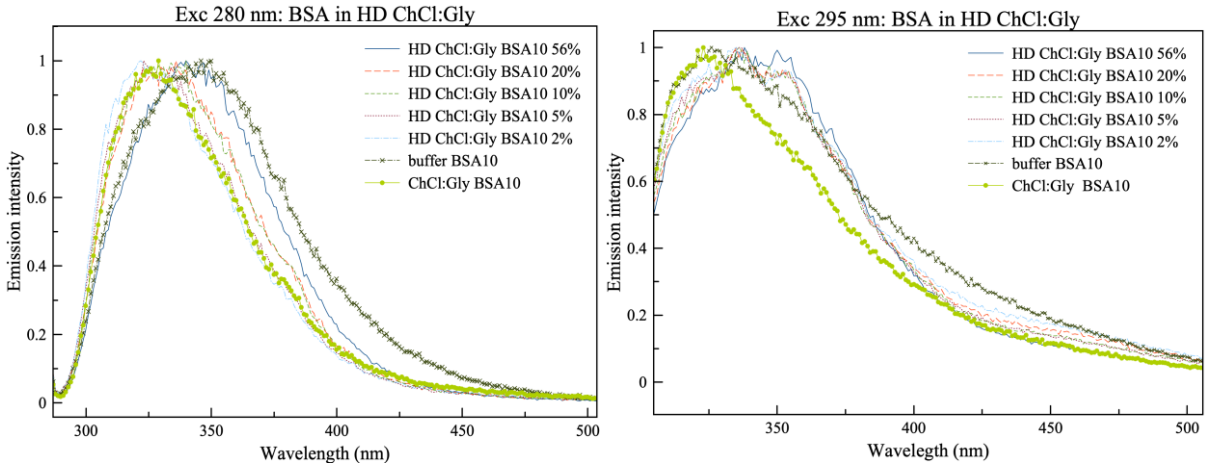

Figure 18. *Normalized emission spectra of BSA10 in HD ChCl:Gly with different wt% water at exc 280 nm (left) and 295 nm (right). Curves for BSA in phosphate buffer (x) and pure ChCl:Gly (・) are also shown.*

Regarding lysozyme in HD ChCl:Gly, no apparent trend is seen for the curves at both excitation wavelengths (280 and 295 nm), *Figure 19*. All of the hydrated samples give rise to similar curves. For excitation at 280 nm, λ_{max} of these curves appears somewhere between λ_{max} of lysozyme in pure ChCl:Gly and lysozyme in buffer. Since the shift of λ_{max} is towards longer wavelengths for lysozyme in HD ChCl:Gly and pure ChCl:Gly (where the shift is bigger for lysozyme in pure ChCl:Gly) compared to the buffer, this indicates that the local structure around the fluorophores is changed to a bigger extent when lysozyme is in pure ChCl:Gly compared to when it is in HD ChCl:Gly. For excitation at 295 nm, lysozyme in HD ChCl:Gly exhibited a λ_{max} similar to that of lysozyme in pure ChCl:Gly, indicating that the local environment of Trp is not changed when water is added to the system. As stated in section 5.4, the conclusions drawn here about the shift in λ_{max} are valid for proteins in aqueous solutions, which HD ChCl:Gly might not be considered as and the conclusions drawn are therefore just suggestions on explanations for the seen results.

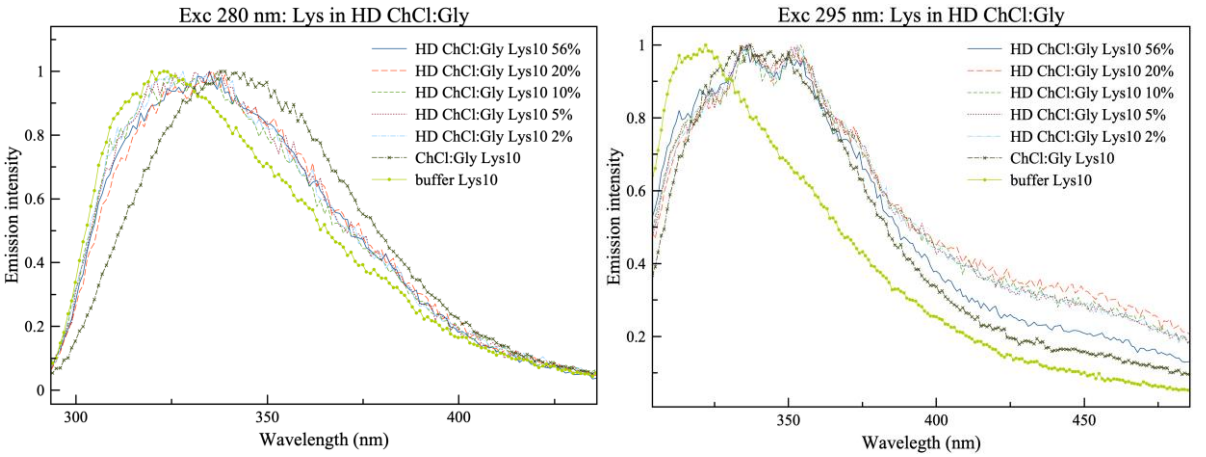

Figure 19. *Normalized emission spectra of Lys10 in HD ChCl:Gly with different wt% water at exc 280 nm (left) and 295 nm (right). Curves for lysozyme in phosphate buffer (x) and pure ChCl:Gly (・) are also shown.*

5.6. Extracted proteins

5.6.1. Extracted proteins: UV-Vis measurements

Before extraction of the proteins to buffer, UV-Vis measurements of the proteins in ChCl:Gly were performed to see if the proteins were degraded or not after 40 days of storage in ChCl:Gly. Both lysozyme and BSA in ChCl:Gly at day 40 exhibit an absorbance similar to the same proteins at day 1 (*Figure 20*), but with a somewhat higher baseline. The normalized curves of these graphs (*Figure 21*) show that the shapes of the peaks are similar as well. The biggest difference between the curves of protein at day 1 and 40 is the intensity at different wavelengths, but since the shapes and positions of shoulders and valleys of the peak are almost the same, it was assumed that the proteins were not degraded after 40 days and extraction of these proteins to buffer could be performed. This is further supported by the first derivatives of the absorbance curves of respective proteins at day 1 and day 40 (*Figure 22*), which are similar to each other.

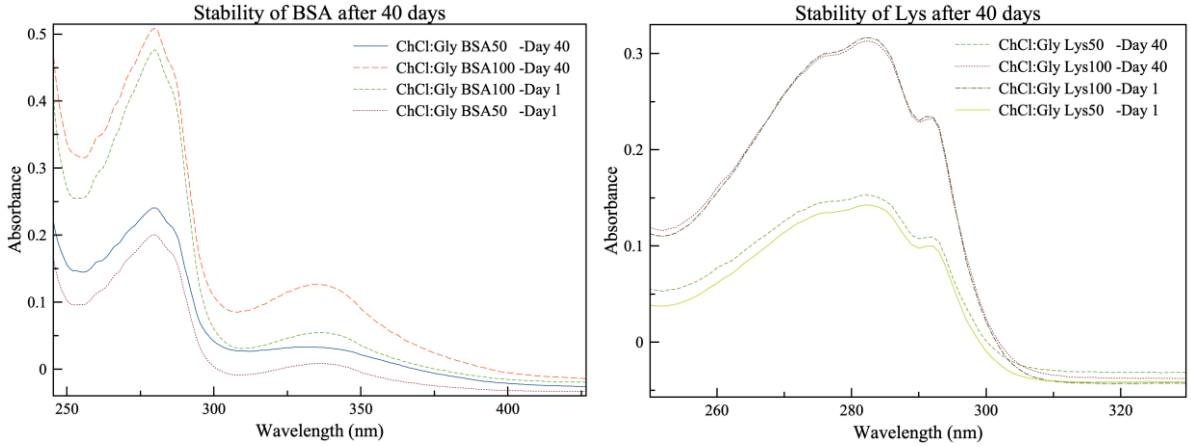

***Figure 20**. Absorbance curves of BSA (left) and lysozyme (right), in the concentrations 50 and 100 μM, in ChCl:Gly at day 1 and day 40.*

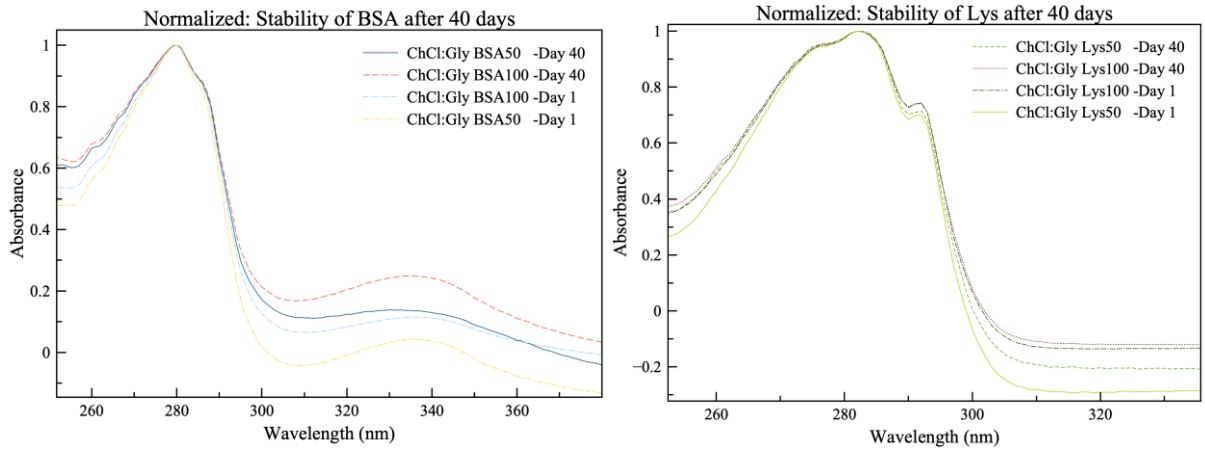

***Figure 21**. Normalized absorbance curves of BSA (left) and lysozyme (right), in the concentrations 50 and 100 μM, in ChCl:Gly at day 1 and day 40.*

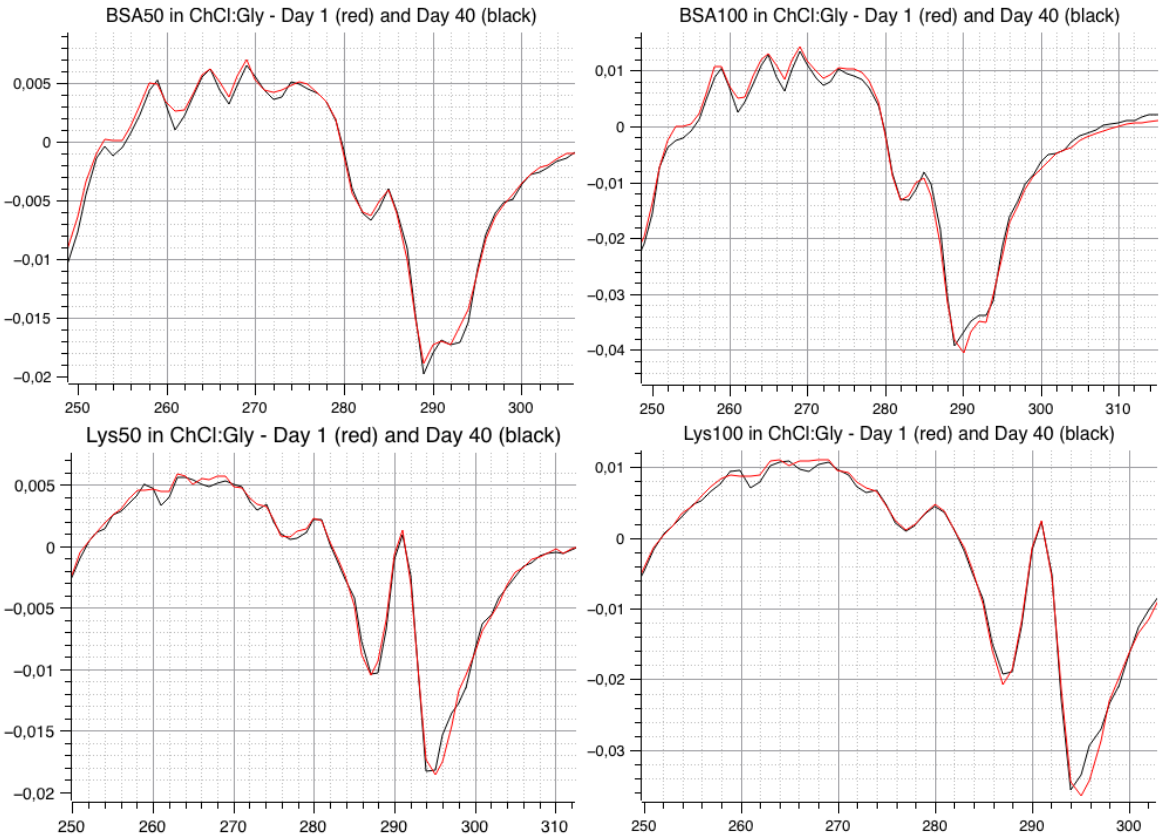

Figure 22. *First derivatives of the absorbance curves for BSA (top) and lysozyme (bottom), in the concentrations 50 and 100 μM, in ChCl:Gly at day 1 and day 40.*

The proteins were diluted during extraction since they were extracted from a smaller volume of ChCl:Gly to an unknown bigger volume of phosphate buffer. The absorbance of extracted protein *(Figure 23)* corresponds to an absorbance of protein between 10-50 μM in the buffer. The curves for the extracted proteins (both BSA and lysozyme) show similar shape both to the curves of protein in buffer and protein in ChCl:Gly (see *Appendix F* for normalized graphs and easier visualization of shapes of the curves). As can be seen from the graph in *Figure 23*, extracted BSA also has an additional peak at 300-400 nm, as BSA in ChCl:Gly. This suggests that BSA might not have regained all of its native conformation or that irreversible interactions between protein and solvent (ChCl:Gly) or solvent components have occurred.

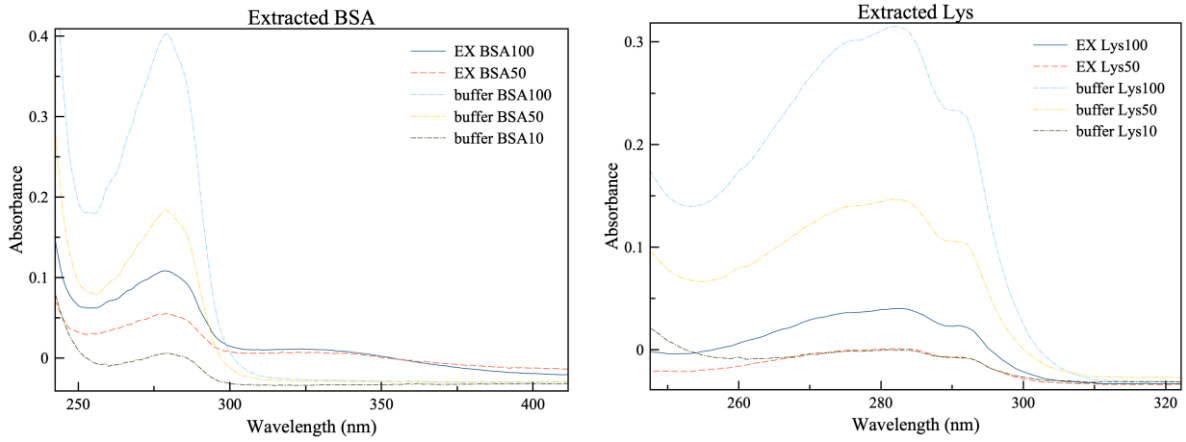

Figure 23. *UV-Vis absorbance of extracted (EX) BSA (left) and lysozyme (right). The extracted proteins exhibit an absorbance that corresponds to a concentration between 10-50 μM in buffer. The curves of extracted protein are similar to the curves of protein in buffer and protein in ChCl:Gly. The peak at 300-400 nm of BSA in ChCl:Gly is still present for extracted BSA.*

5.6.2. Extracted proteins: FT-IR measurements

From the FT-IR graphs of extracted protein (*Figure 24*), it can be seen that the curves for extracted proteins are almost identical to the curves of protein in phosphate buffer. This is reasonable since the proteins were extracted to phosphate buffer and almost no ChCl:Gly is expected to be remaining in the samples after three dialysis cycles. As for the proteins in buffer, the amide I peak is also hidden behind another peak for the extracted proteins and therefore subtraction of the curves with pure buffer has to be made before analysis of the amide I peak. However, after the subtraction, the intensities of the amide I peak was very low resulting in much noise *(Figure 25)* and therefore no valid comparisons could be made. The intensities for the extracted proteins were low because the protein concentrations were low after extraction.

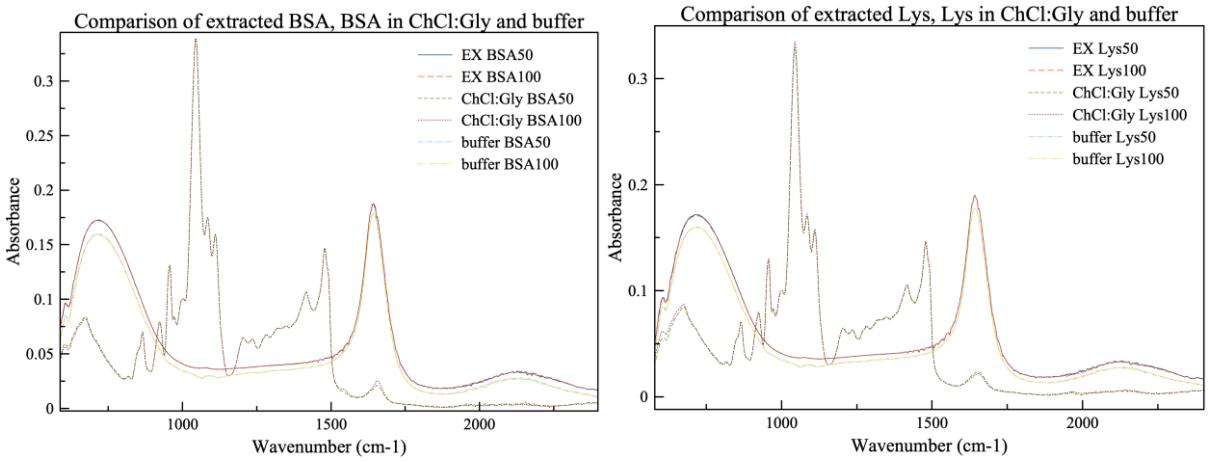

Figure 24. *FT-IR spectra of extracted (EX) BSA (left) and lysozyme (right). The amide I peak can be seen in the wavenumber 1650 cm^{-1}. The curves of extracted proteins are overlapping with the curves of protein in buffer.*

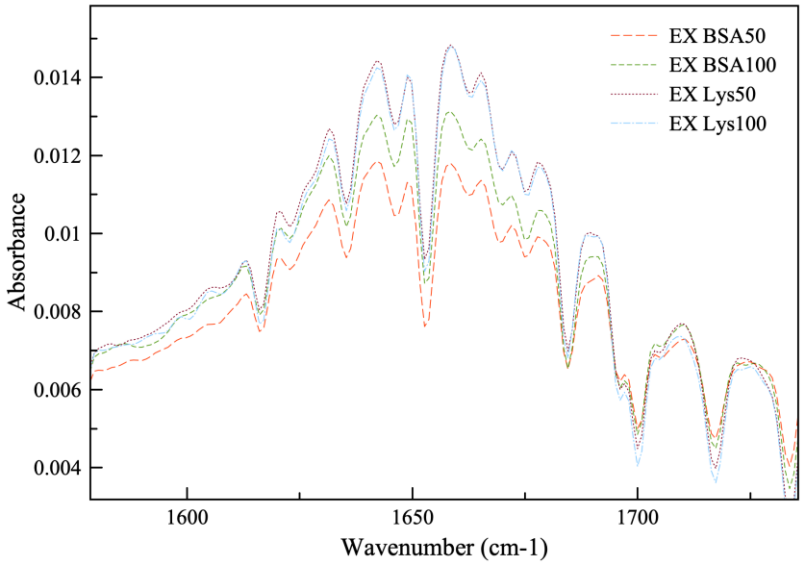

Figure 25. *Zoom of the amide I peak in the curves of extracted (EX) BSA and lysozyme. The curves have been subtracted with the curve of pure phosphate buffer, to be able to analyze the shape of the amide I peak. As can be seen, the resulting curves have very low intensity (max 0.014 absorbance units) after subtraction, making it hard to make valid conclusions about the shape of the amide I peak.*

5.6.3. Extracted proteins: Fluorescence measurements

The normalized emission spectra of extracted BSA compared with normalized emission spectra of BSA in ChCl:Gly and BSA in phosphate buffer (*Figure 26*) do not show uniform results. For excitation at 280 nm, extracted BSA50 and BSA100 exhibit different emission curves with different λ_{max}. These should be similar if no quenching effects (discussed in section 5.4.) are present and if the heights of the volumes were the same. Nevertheless, extracted BSA100 has an emission spectrum that is similar to the spectrum of BSA in phosphate buffer, while extracted BSA50 has a spectrum similar to the spectrum of BSA in ChCl:Gly. For excitation at 295 nm, both extracted BSA50 and BSA100 have similar spectra with somewhat similar λ_{max}. These spectra are in turn similar to the spectra of both BSA in ChCl:Gly and BSA10 in buffer. It is worth noting that BSA10 in buffer had a λ_{max} different than BSA50 and BSA100 in buffer and this might be due to the sources of error discussed in section 5.4.

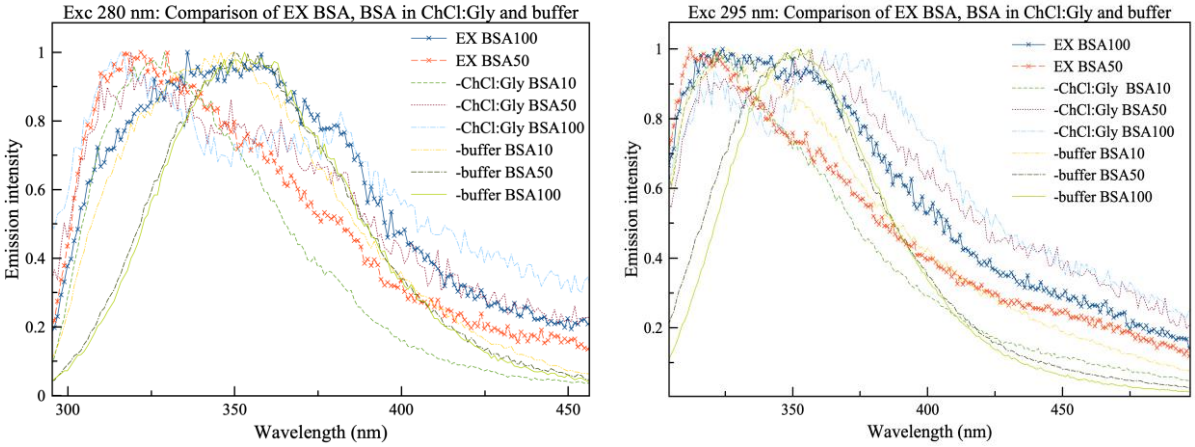

***Figure 26**. Normalized emission spectra of extracted (EX) BSA, at the excitation wavelengths 280 (left) and 295 nm (right), compared with emission spectra of BSA in ChCl:Gly and BSA in phosphate buffer. The spectra of extracted BSA50 and BSA100 are marked with x, for easier visualization.*

For extracted lysozyme, the normalized spectra of extracted Lys50 and Lys100 are similar to each other, both in the excitation wavelength of 280 nm and 295 nm (*Figure 27*). The extracted lysozyme seems to have an emission spectrum that is similar to Lys10 in buffer, suggesting that lysozyme retains most of its native conformation when it is back-extracted from ChCl:Gly to buffer.

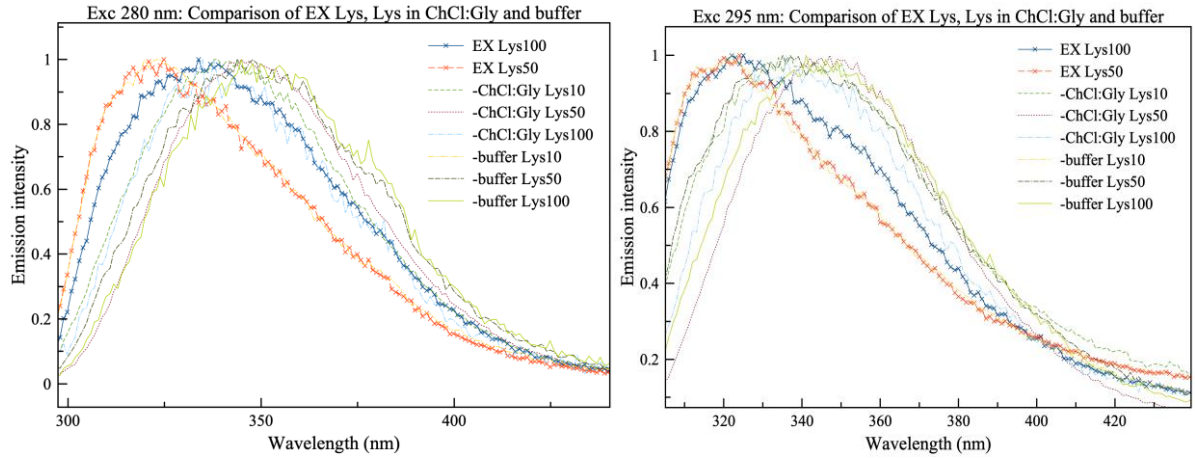

***Figure 27**. Normalized emission spectra of extracted (EX) lysozyme, at the excitation wavelengths 280 (left) and 295 nm (right), compared with emission spectra of lysozyme in ChCl:Gly and lysozyme in phosphate buffer. The spectra of extracted Lys50 and Lys100 are marked with x, for easier visualization. It can be seen, for both excitation wavelengths, that the spectra for extracted lysozyme are similar to the spectra of Lys10 in buffer.*

6. Conclusion

From the measurements, it can be concluded that both BSA and lysozyme have changed conformation when they are in the different DESs. From the UV-Vis measurements, the obtained outcome is that the conformation of BSA and lysozyme seems to be best retained in ChCl:Gly. Since the amide I peak (which is an indication of alpha helices and beta sheets in the proteins) was varied in ChCl:Gly and ChAc:Gly (from the FT-IR measurements), the secondary structures of BSA and lysozyme are altered when the proteins are in these DESs. The emission maximum has clearly shifted as can be seen from the fluorescence measurements. For BSA, the shift in emission maximum can imply that the local environment of the fluorophores has changed to be more a hydrophobic cybotactic region and for lysozyme it was suggested that the local structure of the fluorophores had changed when lysozyme is in DESs. Alternatively, these changes of emission maximum can also be due to changes in the interactions of the proteins with the DESs. The experiments showed that in water-free DESs, the glycerol-containing DESs seemed to stabilize the proteins better than the urea-containing DESs as aggregation was seen in the latter. In difference from ChCl, ChAc gave yellow-coloured samples, particularly after freeze drying. This was not further investigated, but could be a potential problem for ChAc.

When adding water to the ChCl:Gly DES, the native protein conformations were better retained compared to when the proteins are in pure ChCl:Gly. It cannot however be concluded which water content is the most suitable, but the hydrated ChCl:Gly with higher water contents (somewhere below 50 but higher than 20 wt% water) becomes more of an aqueous solution of the DES components rather than a DES. Furthermore, the measurements of the extracted proteins indicate that the proteins regain most of their native conformation when they are transferred back to buffer. However, the additional peak at 300-400 nm in the UV-Vis spectrum of BSA in pure ChCl:Gly was apparent even for the extracted BSA. This is an interesting observation, indicating that BSA might not have regained all of its native conformation or that irreversible interactions between protein and solvent (ChCl:Gly) or solvent components have occurred.

To conclude our observations, deep eutectic solvents might be applicable in drug formulation. However, more studies have to be performed (both on different DESs and proteins as well as more replicates of our studies) to obtain complementing information.

7. Future outlook

Besides using the mentioned techniques to study protein conformation and protein interactions with the environment, there are other techniques that would be useful to further investigate what effects the DESs have on proteins. One example of a technique that would be of importance to complement the obtained data regarding the structure of protein, e. g. by looking more into the secondary structure, is circular dichroism (CD). When planning this master thesis, the initial intent was to perform CD measurements but due to unexpected circumstances, the experiments could not be performed. Additionally, as mentioned in the results, some of the protein samples (particularly the BSA samples in ChAc:Gly) obtained a distinct yellow color after the freeze drying process. Since no control of the conditions were possible during freeze drying, a hypothesis is that the samples might not have been kept frozen and degraded during the process, causing changes in the sample characteristics. Hence, controlled freeze drying could provide a sufficiently low temperature during drying that can avoid boiling of the samples.

Moreover, the results provided by the FT-IR measurements made it difficult to draw any proper conclusions and the fluorescence results did not give consistent data for the different concentrations, which is why it would be preferable if more analysis was conducted for the two particular techniques. An additional complement to this investigation could be to perform activity measurements for lysozyme, for instance before and after extraction of the protein from the DES, in order to analyze if the protein is able to retain its function after it has been exposed to DES. By combining these approaches together with e.g. SAXS/SANS, examination of local structure and dynamics as well as detailed studies of protein conformation would be enabled. Consequently, the understanding of the interactions between proteins and the DESs would be improved.

8. References

Abbott, A. P., Capper, G., Davies, D. L., Rasheed, R. K. and Tambyrajah, V. (2003). Novel solvent properties of choline chloride/urea mixtures. *Chemical Communications*, [online] (1), pp. 70-71. Available at https://pubs.rsc.org/en/content/articlelanding/2003/cc/b210714g#!divAbstract [Accessed 14 Apr. 2020].

Abbott, A. P., Cullis, P.M., Gibson, M.J., Harris, R.C. and Raven E. (2007). Extraction of glycerol from biodiesel into a eutectic based ionic liquid. *Green Chemistry*, 9(8), pp. 868‑872.

Assadpour, E. and Jafari, S.M. (2019). An overview of biopolymer nanostructures for encapsulation of food ingredients. In: Biopolymer Nanostructures for Food Encapsulation Purposes. Elsevier, pp. 10-11.

Barth, A. (2007). Infrared spectroscopy of proteins. *Biochimica et Biophysica Acta (BBA) - Bioenergetics*, 1767(9), pp. 1073-1080.

Berg, M. J., Tymoczko, J. L, Gatto, G. J. and Stryer, L. (2015). Biochemistry. 8th ed. New York: W.H. Freeman and Company, pp. 42-48.

Biological Magnetic Resonance Data Bank, (2017). *BMRB Featured System: Lysozyme.* [online] Available at: http://www.bmrb.wisc.edu/featuredSys/Lysozyme/ [Accessed 20 Mar 2020].

Buxbaum E. (2015) *Protein Structure*. In: Fundamentals of Protein Structure and Function, 2nd ed. Cham: Springer, pp. 15-37.

Dai, Y., van Spronsen, J., Witkamp, G., Verpoorte, R. and Choi, Y. H. (2013). Natural Deep Eutectic Solvents as new potential media for green technology. *Analytica Chimica Acta*, [online] Volume 766, pp. 61-68. Available at https://www.sciencedirect.com/science/article/abs/pii/S0003267012018260 [Accessed 14 Apr. 2020].

Desbois, S. (2013). Some practical guidelines for UV imaging in the protein crystallization laboratory. *Acta Crystallographica*, 69, p. 201.

Durand, E., Lecomte, J., Baréa, B., Dubreucq, E., Lortie, R. and Villieneuve, P. (2013). Evaluation of deep eutectic solvent-water binary mixtures for lipase-catalyzed lipophilization of phenolic acids. *Green Chemistry*, [online] Volume 15(8), pp. 2275-2282. Available at https://pubs.rsc.org/en/content/articlelanding/2013/gc/c3gc40899j#!divAbstract [Accessed 14 Apr. 2020].

Dwivedi, C., Pandey, I., Pandey, H., Ramteke, P.W., Pandey, A.C., Mishra, S.B. and Patil, S. (2017). Chapter 9 - Electrospun Nanofibrous Scaffold as a Potential Carrier of Antimicrobial Therapeutics for Diabetic Wound Healing and Tissue Regeneration. In: *Nano- and Microscale Drug Delivery Systems*, 1st ed. Elsevier, p. 158.

Esquembre, R., Sanz, J. M., Wall, J. G., del Monte, F., Mateo, C. R. and Ferrer, M. L. (2013). Thermal unfolding and refolding of lysozyme in deep eutectic solvents and their aqueous dilutions. *Phys. Chem. Chem. Phys.*, [online] Volume 15(27), pp. 11248-11256. Available at https://pubs.rsc.org/en/content/articlelanding/2013/cp/c3cp44299c#!divAbstract [Accessed 14 Apr. 2020].

Formoso, C. and Forster, L.S. (1975). Tryptophan fluorescence lifetimes in lysozyme. *The Journal of Biological Chemistry*, 250(10), p. 3738.

Gasdia-Cochrane, M. (2018). How Water Affects Raman and FTIR Identification of Unknown Substances. [online] *Thermo Fisher Scientific*. Available at: https://www.thermofisher.com/blog/identifying-threats/how-water-affects-raman-and-ftir-identification-of-unknown-substances/ [Accessed 20 May 2020].

Ghisaidoobe, A.B.T. and Chung, S.J. (2014). Intrinsic Tryptophan Fluorescence in the Detection and Analysis of Proteins: A Focus on Förster Resonance Energy Transfer Techniques. *International Journal of Molecular Sciences*, 15(12), pp. 22518-22521.

Gutiérrez, M. C., Ferrer, M. L., Yuste, L., Rojo, F. and del Monte, F. (2010). Bacteria Incorporation in Deep-eutectic Solvents through Freeze-Drying. *Angew. Chem. Int. Ed.*, [online] Volume 49(12), pp. 2158-2162. Available at https://onlinelibrary.wiley.com/doi/abs/10.1002/anie.200905212 [Accessed 14 Apr. 2020].

Hammond, O. S., Bowron, D. T. and Edler, K. J. (2016). Liquid structure of the choline chloride-urea deep eutectic solvent (reline) from neutron diffraction and atomistic modelling. *Green Chemistry*, [online] 18(9), pp. 2736-2744. Available at: https://pubs.rsc.org/en/content/articlelanding/2016/gc/c5gc02914g#!divAbstract [Accessed 5 June 2020]

Hammond, O. S., Bowron, D. T. and Edler, K. J. (2017). The Effect of Water upon Deep Eutectic Solvent Nanostructure: An Unusual Transition from Ionic Mixture to Aqueous Solution. *Angew. Chem. Int. Ed.*, [online] Volume 56(33), pp. 9782-9785. Available at https://onlinelibrary.wiley.com/doi/full/10.1002/anie.201702486 [Accessed 14 Apr. 2020].

Lapidus, L.J. (2017). Protein unfolding mechanisms and their effects on folding experiments. F1000 Faculty Reviews, 6, pp. 1-2.

Mehmood, A.M., lyer, A.B., Arif, S., Junaid, M., Khan, R.S., Nazir, W. and Khalid, N. (2019) Whey Protein-Based Functional Energy Drinks Formulation and Characterization. In: Sports and Energy Drinks, 1st ed. Elsevier, p. 166.

Möller, M. and Denicola, A. (2002) Protein Tryptophan Accessibility Studied by Fluorescence Quenching. *Biochemistry and Molecular Biology Education*, 30(3), pp. 175-178.

Monhemi, H., Housaindokht, M. R., Moosavi-Movahedi, A. A. and Bozorgmehr, M. R. (2014). How a protein can remain stable in a solvent with high content of urea: insights from molecular dynamics simulation of Candida antarctica lipase B in urea : choline chloride deep eutectic solvent. *Phys. Chem. Chem. Phys.*, [online] 16(28), pp. 14882-14893. Available at https://pubmed.ncbi.nlm.nih.gov/24930496/ [Accessed 14 Apr. 2020].

Owen, A. J. (2000). *Uses of Derivative Spectroscopy Application Note UV-Visible Spectroscopy*. [PDF] Agilent Technologies. Available at https://www.whoi.edu/cms/files/derivative_spectroscopy_59633940_175744.pdf [Accessed 14 Apr. 2020].

Pawar, P.M., Jarag, K.J. and Shankarling, G.S. (2011). Environmentally benign and energy efficient methodology for condensation: an interesting facet to the classical Perkin reaction. *Green Chemistry*, 13(8), pp. 2130-2134.

Peng, Z.G., Hidajat, K. and Uddin, M.S. (2005). Selective and sequential adsorption of bovine serum albumin and lysozyme from a binary mixture on nanosized magnetic particles. *Journal of Colloid and Interface Science*, 281(1), pp. 11-17.

Peters, T. (1995). All About Albumin: Biochemistry, Genetics, and Medical Applications. Academic Press, p. 16.

Phillips, D.C. (1967). The Hen Egg-White Lysozyme Molecule. *Proceedings of the National Academy of Sciences of the United States of America,* 57(3), p. 484.

Prieur, D.J., Olson, H.M. and Young D.M. (1974). Lysozyme Deficiency-An Inherited Disorder of Rabbits. *The American Journal of Pathology*, 77(2), p. 283.

Royer, C. A. (2006). Probing Protein Folding and Conformational Transitions with Fluorescence. *Chemical Reviews*, 106(5), pp. 1769–1784.

Sanchez-Fernandez, A., Edler, K. J., Arnold, T., Alba Venero, D. and Jackson, A. J. (2017). Protein conformation in pure and hydrated deep eutectic solvents. *Phys Chem Chem Phys*, 19(13), pp. 8667-8670.

Sen, R. and Dasgupta, D. (2004). Simple Fluorescence Assays Probing Conformational Changes of Escherichia coli RNA Polymerase During Transcription Initiation. In: *Methods in Enzymology*. Elsevier, p. 601.

Sigma Aldrich. Albumin, bovine. [online] Available at: https://www.sigmaaldrich.com/content/dam/sigma-aldrich/docs/Sigma/Product_Information_Sheet/a4919pis.pdf?fbclid=IwAR3uaZrA55Zug_vzOpdkVFk6pi9Zj-hz7oXzvxqKHJF2B8KN7yoEV4KeVaQ [Accessed 15 Mar 2020].

Sigma Aldrich. Bovine Serum Albumins. [online] Available at: https://www.sigmaaldrich.com/life-science/biochemicals/biochemical-products.html?TablePage=103994915 [Accessed 15 Mar 2020].

Sigma Aldrich. *Lysozyme from chicken egg white*. [online] Available at: https://www.sigmaaldrich.com/catalog/product/sigma/l6876?lang=en&region=SE [Accessed 15 Mar 2020].

Singh, B., Lobo, H. and Shankarling, G. (2011). Selective N-Alkylation of Aromatic Primary Amines Catalyzed by Bio-catalyst or Deep Eutectic Solvent. *Catalysis Letters*, 141, p. 182.

Smith, E.L., Abbot A.P. and Ryder, K.S. (2014). Deep Eutectic Solvents (DESs) and Their Applications. *Chemical Reviews*, 114(21), pp. 11074-11076.

Strosberg, A.D., Van Hoeck, B. and Kanarek, L. (1971). Immunochemical Studies on Hen's Egg-White Lysozyme. *The FEBS Journal*, 19(1), p. 36.

Worsfold, P. J. and Zagatto, E. A. G. (2019). Spectrophotometry | Overview. In: P. Worsfold, A. Townshend, C. Poole and M. Miró, ed., *Encyclopedia of Analytical Science*, 3rd ed. Volume 9, Elsevier, pp. 244-248.

Zhang, Q., De Oliveira Vigier, K., Royer, S. and Jérôme, F. (2012). Deep eutectic solvents: syntheses, properties and applications. *Chem. Soc. Rev*, [online] Volume 41(21), pp. 7108-7146. Available at: https://pubs.rsc.org/en/content/articlelanding/2012/CS/c2cs35178a#!divAbstract [Accessed 14 Apr. 2020].

Zhang, Q., Vigier, K., Royer, S. and Jerome F. (2012). Deep eutectic solvents: syntheses, properties and applications. *Chemical Society Reviews*, 41(21), p. 7118.

9. Appendices

Appendix A. Calculations for DESs in molar ratio 1:2

ChCl:Gly (1:2)

$MW_{ChCl} = 139.62\ g/mol$
$MW_{Gly} = 92.09\ g/mol$

$m = M * n$

$m_{tot} = 50\ g = m_{ChCl} + m_{Gly} = 139.62 * n + 92.09 * 2n = 323.8\ n \Leftrightarrow n = 0.15442\ mol$

$\Rightarrow m_{ChCl} = 139.62 * 1n = 21.56012\ g$
$\Rightarrow m_{Gly} = 92.09 * 2n = 28.44108\ g$

ChCl:U (1:2)

$MW_{ChCl} = 139.62\ g/mol$
$MW_{U} = 60.06\ g/mol$

$m = M * n$

$m_{tot} = 50\ g = m_{ChCl} + m_{U} = 139.62 * n + 60.06 * 2n = 259.74n \Leftrightarrow n = 0.19250019\ mol$

$\Rightarrow m_{ChCl} = 139.62 * 1n = 26.8768765\ g$
$\Rightarrow m_{U} = 60.06 * 2n = 23.1231228\ g$

ChAc:Gly (1:2)

$MW_{ChAc} = 163.21\ g/mol$
$MW_{Gly} = 92.09\ g/mol$

$m = M * n$

$m_{tot} = 50\ g = m_{ChAc} + m_{Gly} = 163.21 * n + 92.09 * 2n = 347.39\ n \Leftrightarrow n = 0.1439304528\ mol$

$\Rightarrow m_{ChAc} = 163.21 * 1n = 23.4908892\ g$
$\Rightarrow m_{Gly} = 92.09 * 2n = 26.5091108\ g$

Appendix B. Calculations for the protein stock solutions

1000 μM BSA in H_2O

$MW_{BSA} = 66\,400\ g/mol$

$$n = \frac{m}{M} = c * V$$

Calculations for 1 mL:

$$n = c * V = 1000 * \frac{10^{-6} mol}{L} * 10^{-3} L = 10^{-6} mol$$

$$m = n * M = 10^{-6} * 66400 = 0.0664\ g$$

1000 μM Lysozyme in H_2O

$MW_{lysozyme} = 14\,300\ g/mol$

$$n = \frac{m}{M} = c * V$$

Calculations for 1 mL:

$$n = c * V = 1000 * \frac{10^{-6} mol}{L} * 10^{-3} L = 10^{-6} mol$$

$$m = n * M = 10^{-6} * 14300 = 0.0143\ g$$

Appendix C. Preparation of hydrated ChCl:Gly samples – added amounts

HD DES: protein concentration of 50 µM

Hydrated DES calculations for a total weight of 5g with water contents of 2, 5, 10, 20 and 50 wt%.

Assuming:

$$\rho_{H_2O} = \rho_{protein\ solution} = \frac{1000g}{L} = \frac{1g}{mL}$$

H_2O (wt%)	DES (g)	Milli-Q (g)	Protein solution (g)
2	4.90	0	0.1
5	4.75	0.15	0.1
10	4.5	0.40	0.1
20	4.0	0.90	0.1
50	2.5	2.40	0.1

Protein solution: Proteins in the concentration of 2500 µM in Milli-Q (50x dilution of these protein solutions was made when added to the hydrated DES (e.g. 2500 µM in Milli-Q –> 50 µM in hydrated DESs).

HD DES: protein concentration of 10 µM

Hydrated DES calculations for a total weight of 5g with water contents of 2, 5, 10, 20 and 56 wt%.

Assuming:

$$\rho_{H_2O} = \rho_{protein\ solution} = \frac{1000g}{L} = \frac{1g}{mL}$$

H_2O (wt%)	DES (g)	Milli-Q (g)	Protein solution (g)
2	4.90	0.05	0.05
5	4.75	0.20	0.05
10	4.5	0.45	0.05
20	4.0	0.95	0.05
56	2.5	2.45	0.05

Protein solution: Proteins in the concentration of 1000 µM in Milli-Q (100x dilution of these protein solutions was made when added to the hydrated DES (e.g. 1000 µM in Milli-Q –> 10 µM in hydrated DESs).

Appendix D. Normalized graphs of the UV-Vis measurements

Normalized curves from the UV-Vis measurements are shown below, for easier comparison of the shapes of the curves.

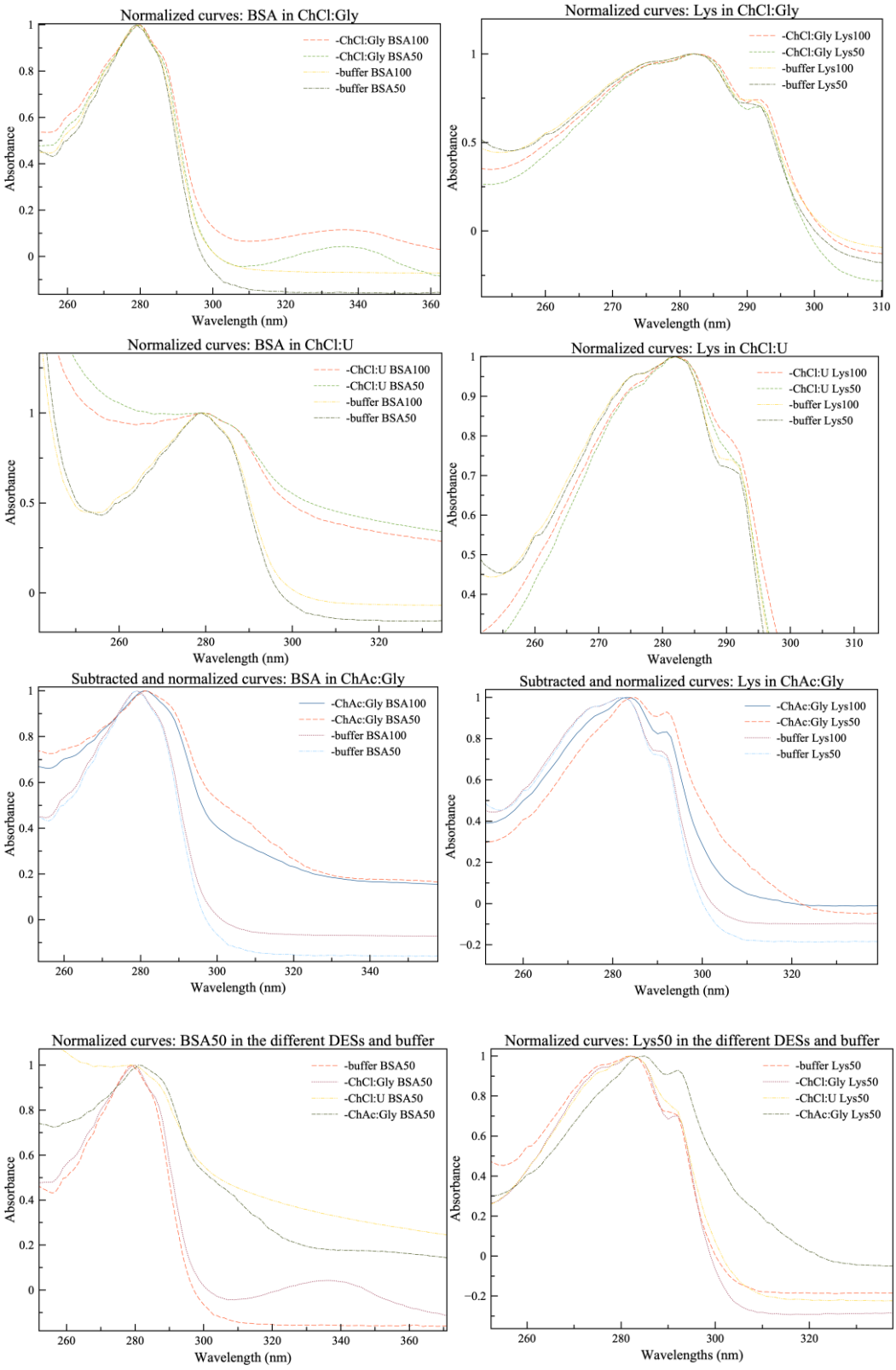

Appendix E. Fluorescence measurement graphs

Graphs obtained from the fluorescence measurements, showing the different emission intensities.

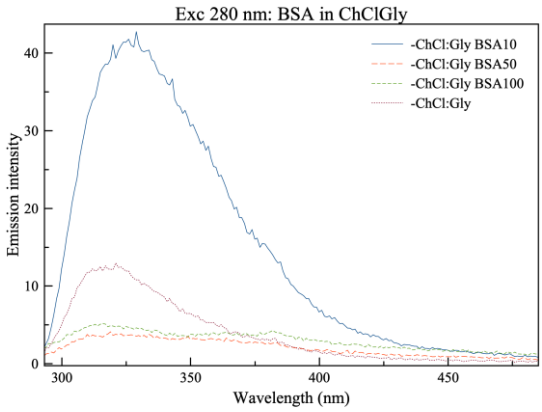

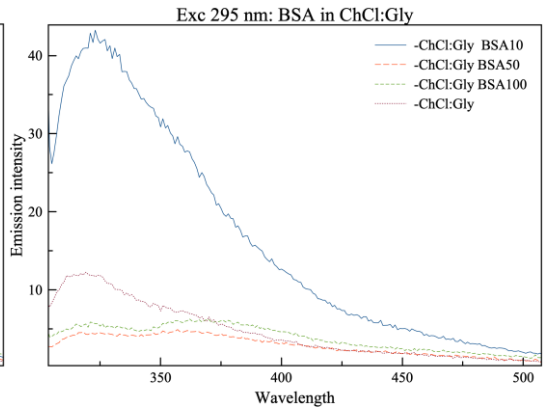

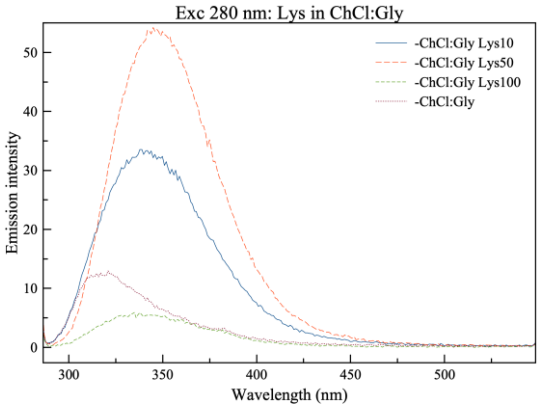

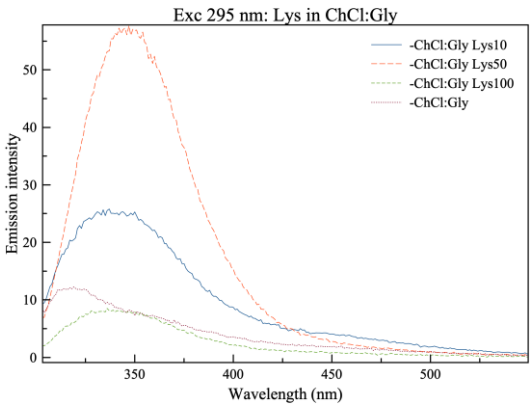

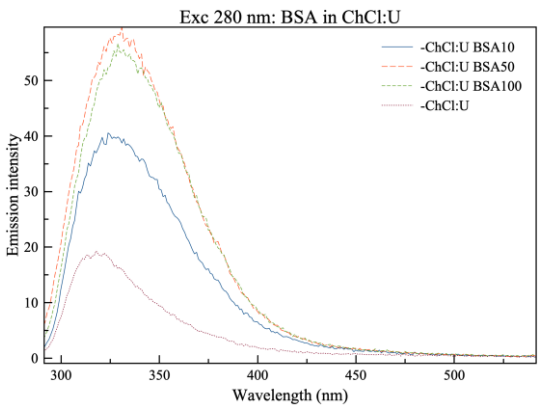

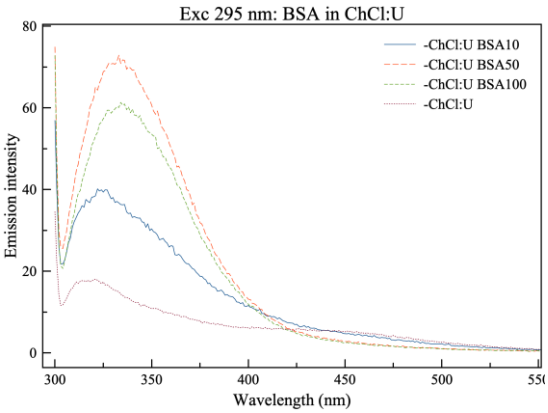

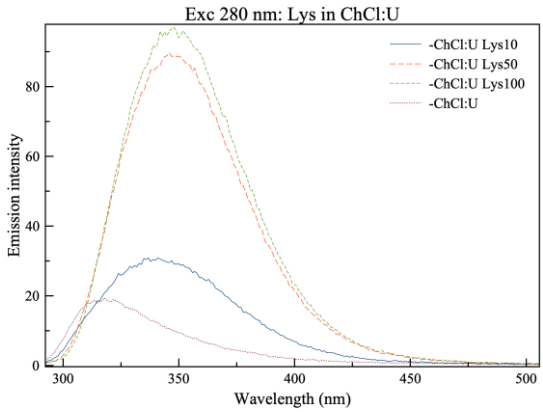

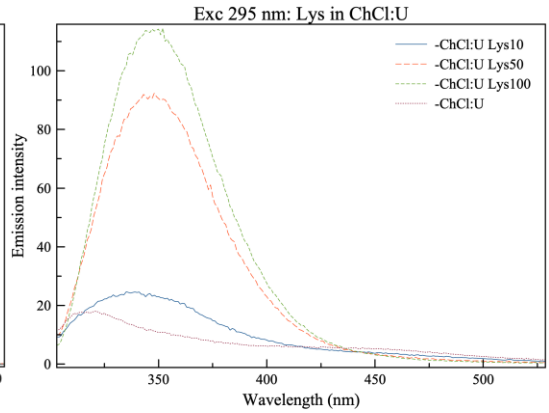

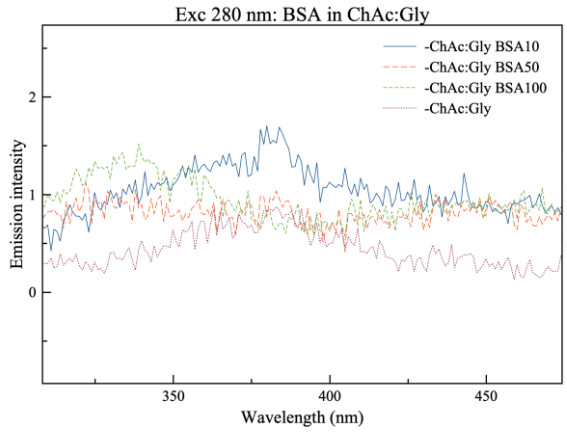
Exc 280 nm: BSA in ChAc:Gly
-ChAc:Gly BSA10
-ChAc:Gly BSA50
-ChAc:Gly BSA100
-ChAc:Gly
Emission intensity
Wavelength (nm)

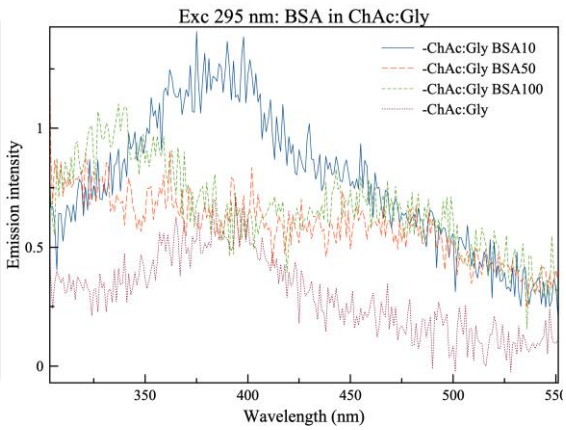
Exc 295 nm: BSA in ChAc:Gly
-ChAc:Gly BSA10
-ChAc:Gly BSA50
-ChAc:Gly BSA100
-ChAc:Gly
Emission intensity
Wavelength (nm)

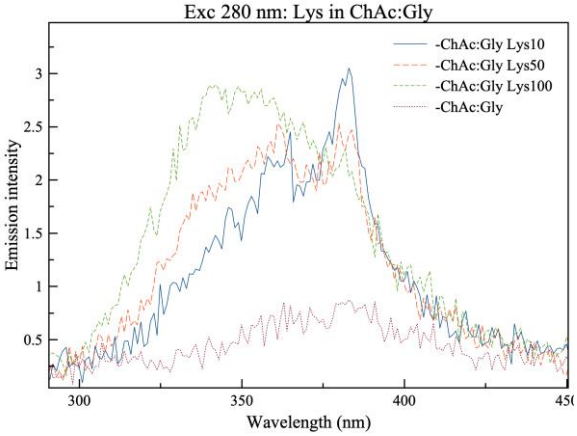
Exc 280 nm: Lys in ChAc:Gly
-ChAc:Gly Lys10
-ChAc:Gly Lys50
-ChAc:Gly Lys100
-ChAc:Gly
Emission intensity
Wavelength (nm)

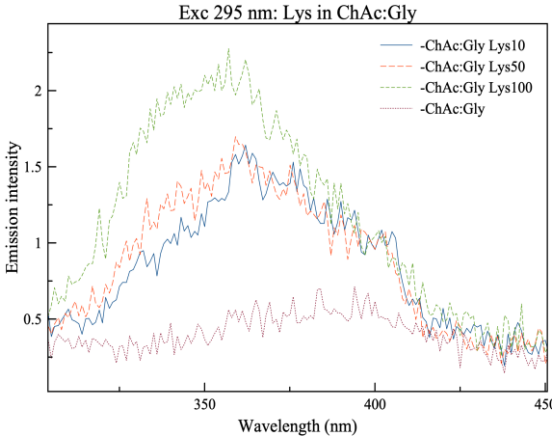
Exc 295 nm: Lys in ChAc:Gly
-ChAc:Gly Lys10
-ChAc:Gly Lys50
-ChAc:Gly Lys100
-ChAc:Gly
Emission intensity
Wavelength (nm)

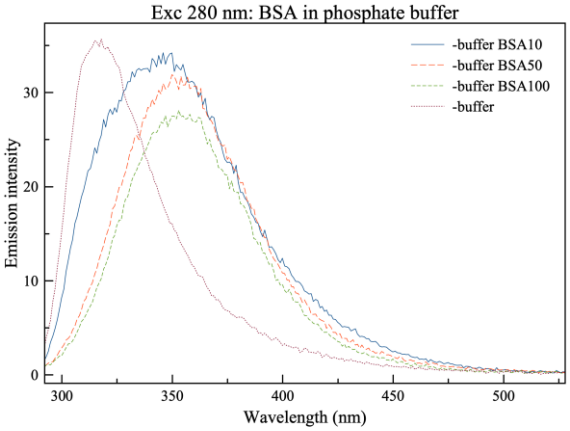
Exc 280 nm: BSA in phosphate buffer
-buffer BSA10
-buffer BSA50
-buffer BSA100
-buffer
Emission intensity
Wavelength (nm)

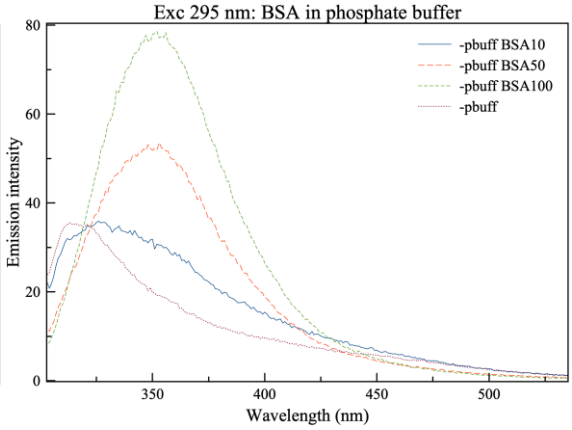
Exc 295 nm: BSA in phosphate buffer
-pbuff BSA10
-pbuff BSA50
-pbuff BSA100
-pbuff
Emission intensity
Wavelength (nm)

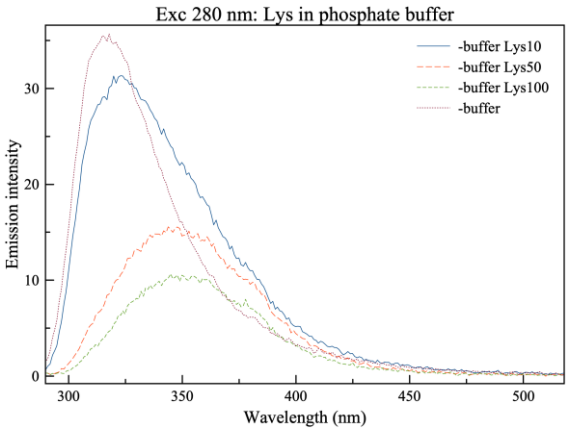
Exc 280 nm: Lys in phosphate buffer
-buffer Lys10
-buffer Lys50
-buffer Lys100
-buffer
Emission intensity
Wavelength (nm)

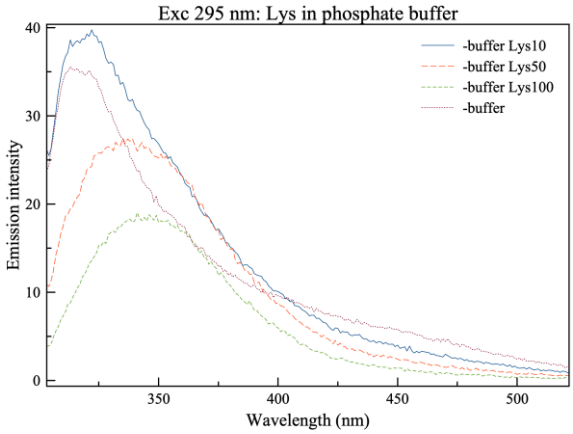
Exc 295 nm: Lys in phosphate buffer
-buffer Lys10
-buffer Lys50
-buffer Lys100
-buffer
Emission intensity
Wavelength (nm)

Appendix F. Normalized UV-Vis graphs of extracted protein

Normalized curves of extracted BSA and lysozyme, BSA and lysozyme in ChCl:Gly and BSA and lysozyme in phosphate buffer, for comparison of shapes of the curves.